## THE DEVELOPMENT OF A WIRE MARK METER

bу

R.A. Lindsay, B.A.Sc.

A thesis submitted to the Faculty of Graduate Studies and Research in partial fulfilment of the requirements for the degree of Master of Engineering.

Department of Electrical Engineering, McGill University, Montreal.

#### ABSTRACT

An instrument based on the Chapman Printing Smoothness Tester has been devised to measure the distribution of paper surface roughness variations in the wavelength region between 1/6 and 1/90 of an inch. The measurement is made by scanning a small spot of light over the contact interface between a smooth glass block and the paper surface. Light scattered from the interface at a shallow angle is proportional to the area of optical contact lying within the spot, and is detected by a sensitive photomultiplier tube. A frequency analysis of this time-varying photomultiplier signal yields a band-limited noise spectrum corresponding to the random distribution of optical contact areas, along with distinct peaks at the frequencies corresponding to the regular patterns of the woven wire screen upon which the paper was initially formed. (the wire mark). A quantitative assessment of the wire mark intensity may be made by taking the ratio of the average component of the photomultiplier tube signal at the frequency of the wire mark pattern to the total average value of the signal.

Surface roughness spectra may be taken with the instrument on both the top and wire sides of paper samples under pressure, and in both the machine and cross-machine directions of the paper.

Typical surface roughness spectra of Canadian newsprint papers having a wide range of wire marks are illustrated, and the effect of the applied pressure on the surface roughness spectrogram is shown. Also included is a detailed discussion of the problem of assigning a specific wire mark value to a paper sample on the basis of its surface roughness spectrogram.

## ACKNOWLEDGEMENTS

The author wishes to thank Mr. J.G. Buchanan of the Pulp and Paper Research Institute of Canada and Dr. G.L. d'Ombrain of the Department of Electrical Engineering of McGill University for their kind supervision and guidance in this project. He would also like to acknowledge the suggestions and advice of various members of the staff of the Pulp and Paper Research Institute of Canada, in particular Mr. S.M. Chapman and Mr. T.S. Duchnicki.

The assistance of Miss P. Stephen in the preparation of this manuscript deserves special mention.

Above all, the author is especially grateful for the co-operation of the Department of Electrical Engineering and the Pulp and Paper Research Institute of Canada which has made this thesis project possible.

# TABLE OF CONTENTS

	Page
TITLE	
ABSTRACT	i
ACKNOWLEDGEMENTS	ii
TABLE OF CONTENTS	iii, iv, v, vi, vii
I : INTRODUCTION	1
1.1 The Problem of Wire Mark	1
1.2 The Measurement of Wire Mark	2
II : BASIC PROPOSALS	4
2.1 Specifications for the Wire Mark Meter	4
2.2 The Operating Principle of the Chapman Printing Smoothnes Tester	s 5
2.3 Scanning of the Paper-to-Glass Contact Interface	6
2.4 The Proposed Definition of a Wire Mark Index	9
2.5 The Effect of the Average Fractional Area of Contact on the Proposed Wire Mark Index	10
2.6 The Choice of a Scanning Waveform	11
2.6.1 Sawtooth Scanning Waveforms	12
2.6.2 Triangular Scanning Waveforms	12
2.7 The Problem of the Frequency Stability of the X-Axis	13

		<del>-</del> '	
			Page
2.8		imitation Imposed on the Size of the Scanning Light	14
2.9		imitation Imposed on the Selectivity of the Filtering	14
2.1	O The T	ime Required to Completely Scan a Paper Sample	15
2.1	1 The E	rror in the Observed Wire Mark Frequency	16
2.1	2 The Cl	noice of a Scanning Method	17
2.1	3 The Cl	noice of a Photodetector	17
2.1	4 The Pi	roposed Block Diagram of the Wire Mark Meter	18
	2.14.	L Generation of the Scanning Raster	18
	2.14.2	2 Detection of the Reflected Light Signal	18
	2.14.3	3 Analysis of the Photodetector Signal	18
	2.14.	4 Output Display	19
III :	IMPLEMEN	VTATION OF HARDWARE	20
3.1		ions of the Electronic Systems of the Wire Mark	20
	3.1.1	The P.M. Tube High Voltage Power Supply	20
	3.1.2	The C.R. Tube High Voltage Power Supply	20
	3.1.3	The C.R. Tube Deflection Yoke	21
	3.1.4	Low Voltage Power Supplies	21
3.2	The So	can Generation Circuitry of the Wire Mark Meter	21
	3.2.1	The Generation of Triangular Wave Sweep Waveforms	22
	3.2.2	The Generation of Complementary Square Wave Signals	22
	3.2.3	The Choice of Triggering Oscillator	23
	3.2.4	The Correspondence Between Actual and Desired Sweep Waveforms	23

				_
		3.2.5	Linearization of the Output Current Waveforms	Page 25
		3.2.6	Fail-Safe Design Features Incorporated into the Sweep Circuitry	26
		3.2.7	Adjustment of the Peak and Average Values of the Deflection Currents	26
	3.3	Contro	l Circuitry of the Wire Mark Meter	27
	3.4	Protec	tive and Safety Circuitry of the Wire Mark Meter	28
	3.5	The An	alysis Circuitry of the Wire Mark Meter	28
		3.5.1	Connection to the Photomultiplier Tube	29
		3.5.2	The Video Amplifier	30
		3.5.3	The Averaging Amplifier	30
		3.5.4	The Filtering Amplifier	31
		3.5.5	Operation of the Analysis Circuitry	33
		3.5.6	External Calibrating Circuitry	35
IV	: Œ	neral d	ISCUSSION	<b>3</b> 6
	4.1	The La	ck of Resolution in the Initial Results	<b>3</b> 6
		4.1.1	Measurement of the Bandwidth of the Photodetector System	37
		4.1.2	Measurement of the Effective Spot Size of the Scanning Light Spot	37
	4.2	Improv	ements in the Optical System	38
		4.2.1	Disadvantages of the Rebuilt Optical System	39
	4.3	Improv	ements in the X and Y Sweep Circuitry	40
	4.4	The Pr	oblems of Thermal Drift	40
	4.5	The Fa	ults in the Filtering Amplifier Circuitry	41
	4.6	Capabi	lities of the Completed Instrument	42

			Page
V	V : EXPERIMENTAL RESULTS		
	5.1	Typical Surface Roughness Spectra of Newsprint	43
		5.1.1 Characteristics of Top Side Spectra	44
		5.1.2 Characteristics of Wire Side Spectra	44
	5.2	The Choice of a Wire Mark Index	46
		5.2.1 The Correlation of Wire Mark Meter Readings with Visual Grading	46
		5.2.2 Theoretical Considerations in the Choice of a Wire Mark Index	49
	5.3	Additions to the Wire Mark Meter	53
	5.4	The Effect of Prism Pressure on the Surface Roughness Spectrum of Newsprint	53
	5.5	Reproducibility of Surface Roughness Spectra at a Single Location	55
VI	: DI	SCUSSION, POSSIBLE IMPROVEMENTS, AND CONCLUSION	58
	6.1	General Discussion	58
	6.2	Possible Improvements to the Wire Mark Meter	59
		6.2.1 Possible Improvements in the Optical System of the Wire Mark Meter	59
		6.2.2 Possible Improvements in the Hydraulic System	60
		6.2.3 Possible Improvements to the Scan Generation Circuitry	61
		6.2.4 Possible Improvements in the Analysis Circuitry	64
	6.3	Conclusion	66
BI	BLIOG	RAPHY	67

- v11 -	
	Page
FIGURES	68-91
List of Figures	68

92-100

92

APPENDIX I : CIRCUIT DIAGRAMS.....

List of Circuit Diagrams.....

#### I : INTRODUCTION

## 1.1 The Problem of Wire Mark

One of the major factors limiting the speed of newsprint paper machines in Canada is the problem of wire mark, which is the imprint left on the underside of paper when it is formed by draining a suspension of papermaking fibres through a moving woven wire screen in the Fourdrinier papermaking process. Because this woven wire screen (the Fourdrinier wire) generally has a different number of strands per inch in the direction in which the machine runs (the machine direction) from the number of strands per inch in the opposite direction, (the cross-machine direction); wire mark patterns have two different fundamental wavelengths. For example, the underside of paper made on a typical newsprint machine with a 68 x 52 mesh Fourdrinier wire will exhibit a periodic surface variation with a wavelength of 1/52 inch in the machine direction and 1/68 inch in the cross-machine direction. The intensity of the wire mark pattern left on the finished paper is determined not only by the physical properties of the individual fibres in the paper machine stock, but also by the pressure-temperature-time history of the stock from the time it first impinges on the Fourdrinier wire to the time it leaves the last calender roll. Little can be done to assess the importance of the various factors involved in the creation of wire mark until an instrument has been devised to measure it.

Although generated on the paper machine, wire mark manifests itself as a problem primarily by interfering with the desired ink distri-

bution in the wire side printing of the finished paper. Because of its periodic nature, even a weak wire mark pattern is easily recognized by the human eye.

## 1.2 The Measurement of Wire Mark

The method adopted for the measurement of wire mark will be necessarily determined by the way in which wire mark is defined. Perhaps the most basic definition is the extent to which the substance of the sheet is arranged in the regular pattern of the Fourdrinier wire. The method of Parker and Attwood 1) involving multiple transmission β-radiographs is based on this definition. By means of successive translations of the paper between exposures, a photographic negative is obtained which may be scanned by an optical densitometer to form an estimate of the periodic component of small scale basis weight variations. The method is time-consuming and does not lend itself to the rapid comparison of large samples.

A second method based on the above definition involves viewing the sheet by transmitted light and measuring the component of transmission intensity variations at the wire mark frequency. The Q.N.S/M. Formation Tester described by Burkhard et al. <sup>2)</sup> may be used to assess wire mark in this way, although with severely limited spatial resolution. The optical transmission method has several attendant drawbacks, in that it cannot be used on opaque or coated papers and cannot differentiate between the top and wire sides of a sheet. In addition, the Q.N.S/M. instrument does not measure wire mark as seen by a printing press, in that the measurement is

not performed while the paper is under pressure. Attempts to examine a printed sheet for wire mark by reflected light with a modified Q.N.S/M. Formation Tester 3) have been further complicated by the introduction of inking variables into the test procedure.

An alternative view of wire mark to that proposed above is based on the postulate that wire mark interferes with printing because it is a property of the wire side surface of the paper. Wire mark might be defined then as the extent to which the contact area between the paper and a completely smooth surface is distributed at the wire mark spacing. Prior to the inception of this project, no instruments to measure wire mark on the basis of this latter definition were known to exist.

## II : BASIC PROPOSALS

## 2.1 Specifications for the Wire Mark Meter

As the first step in the design of an instrument to measure wire mark by a determination of the periodic component in the distribution of contact area between a paper sample and a smooth hard surface, the following list of specifications was drawn up:-

- a) the instrument was to be able to measure wire mark over the spatial frequency range of 1/10 to 1/100 of an inch, and to be able to differentiate clearly between machine direction and cross-machine direction wire marks;
- b) the method was to be applicable to opaque or coated papers,
   but was not to include printing of the paper as a mandatory
   part of the test procedure;
- c) the measurement was to be made over an area of at least one square inch while the paper was subjected to pressures typical of those encountered in the printing process.

All of the above specifications could be met it was felt, by the suitable modification of a Chapman Printing Smoothness Tester, 4) an optical instrument used to determine the average fractional area of contact between a paper sample and smooth glass prism under pressure.

During the early development of the latter instrument it was noted by Chapman <sup>5)</sup> that paper surfaces with the same average fractional area of contact might have that contact area distributed in different

ways: in large irregular areas; in small irregular areas; or, in the case of a heavily wire-marked sample, in areas regularly spaced at the wire mark frequency.

A photograph of a heavily wire-marked newsprint sample as seen through the inspection port of the Chapman Printing Smoothness Tester is given in Figure 1. The prominent machine direction wire mark of this sample appears as a series of parallel bars about 3/8 of an inch apart running from the top to the bottom of the photograph. Due to the optical properties of the paper-to-glass interface, points of optical contact appear bright, while regions of nonoptical contact remain dark. The explanation for this phenomenon may be found from the diagram of the optical system of the Chapman Printing Smoothness Tester given in Figure 2.

#### 2.2 The Operating Principle of the Chapman Printing Smoothness Tester

In the Chapman Printing Smoothness Tester, the paper sample to be measured is clamped between the upper glass compound prism and the lower glass backing plate by hydraulic pressure applied from below. A tungsten filament light bulb floods the sample from above with a condensed beam of white light, while two independent phototubes mounted opposite separate faces of the compound prism observe the sample from two different angles. Light falling on the paper and reflected back upwards through points of optical control can reach both phototubes, because the indices of refraction of the paper and glass are almost the same. Light reflected back upwards at points of nonoptical contact however, (where the actual

interface is air-to-glass, rather than paper-to-glass), undergoes strong refraction due to the difference in the refractive indices of air and glass, and is confined to a 41° cone around the normal at those points. The upper phototube, located within a 41° cone for all points on the sample, can thus see light reflected from the entire paper-to-glass interface; while the lower phototube, located outside a 41° cone for all points on the sample, can see light only from points of optical contact. Because the intensity of illumination at both phototubes is proportional to the intensity of the incident illumination and to the brightness of the paper sample, the fractional area of contact between the paper and the glass may be derived from a relatively simple equation involving only two instrument constants and the ratio of the phototube currents. 5)

#### 2.3 Scanning of the Paper-to-Glass Contact Interface

From the above description of the operating principle of the Chapman Printing Smoothness Tester, it is apparent that by scanning a small point source of light in a timewise-linear fashion over the paper-to-glass contact interface, an electrical signal g(x) may be derived from the lower phototube representing the intensity of light reflected from the interface at the position x. The instantaneous magnitude of g(x) will be proportional to the local intensity of illumination incident on the paper sample l(x); to the area of the scanning light spot A; to the local brightness of the paper b(x); to the local fractional area of contact within the light spot k(x); and to the luminous sensitivity of the photo-

detector M. Thus, we may write

$$g(x) = A \cdot M \cdot l(x) \cdot b(x) \cdot k(x)$$

However, since scanning of the sample is performed at a constant velocity  $v=\frac{x}{t}$ , we may equally well consider the photodetector signal as the time function

$$g(t) = A \cdot M \cdot l(t) \cdot b(t) \cdot k(t)$$

The time average, or D.C. value, of this signal which is given

bу

$$I = \frac{1}{T} \int_{0}^{T} g(t) dt$$

will then be proportional to the average brightness of the paper, B; to the average intensity of illumination, L; to the luminous sensitivity of the photodetector, M; to the scanning spot size, A; and finally to the average fractional area of contact of the paper with the prism, K. Thus we may write  $I = C_1 \cdot B \cdot L \cdot M \cdot A \cdot K \cdot$ 

In order to determine the magnitude of the various periodic components of g(t), the signal g(t) may be passed through a bandpass filter network whose response to a unit impulse input is h(t). The filter network output then will be given by

$$j(t) = \int_0^t g(t-\lambda) \cdot h(\lambda) \cdot d\lambda$$

Because j(t) is the output of a bandpass filter however, it will necessarily have zero mean value: i.e.

$$\lim_{T\to\infty}\frac{1}{T}\int_{0}^{T}j(t)\cdot dt=0$$

One possible way of measuring j(t) is to take its absolute value by fullwave rectification; i.e. let

$$p(t) = \overline{j(t)}$$

and then to take the time-average value of p(t):

$$i = \frac{1}{T} \int_{0}^{T} p(t) dt$$

Because the processes of filtering, full-wave rectification, and averaging are all linear processes, (in the sense that for each process the output amplitude is directly proportional to the input amplitude), the value of i will be proportional to the same factors as was the original time function g(t), but in addition, the magnitude of i will be strongly influenced by the characteristics of the bandpass filter network. In order to perform a meaningful frequency analysis of the signal g(t) then, it is essential that the mid-band gain and Q of the filter network be kept constant for all values of the mid-band frequency. If the latter requirement can be met, then we may write

where  $W_{f}$  represents the time-average value of the rectified components of g(t) that are passed by a filter of mid-band frequency f.

It is apparent then that the ratio of the average rectified filtered signal to the average value of signal

$$i_{f/I} = \frac{c_2 \cdot B \cdot L \cdot M \cdot A \cdot K \cdot W_f}{c_1 \cdot B \cdot L \cdot M \cdot A \cdot K} = c_3 W_f$$

will be proportional to the component of g(t) lying within the passband of the filter; but will be independent of the intensity of illumination, L; the average brightness of the paper sample, B; the luminous sensitivity of the photodetector, M; the size of the scanning light spot, A; and the average fractional area of contact, K.

The signal g(t) however, is a time-wise linear representation of the spatial distribution of contact between the paper sample and the glass prism, and thus the spectrum of contact area distribution for a given paper sample may be obtained by performing a frequency analysis of g(t) in the manner outlined above. The magnitude of the spectrum at the frequency corresponding to the wire mark wavelength could then be expected to give a quantitative assessment of wire mark. It must be borne in mind however, that the spatial wavelength range which may be analyzed will have both upper and lower bounds. The upper frequency limit will be set by the size of the scanning light spot, A, (since no detail may be resolved on the paper surface which is smaller than the effective spot size); while the lower frequency limit will be governed by the minimum number of cycles which appear in the course of a single scan of the sample.

## 2.4 The Proposed Definition of a Wire Mark Index

On the assumption that the paper surface could be repetitively scanned every T seconds, a formal definition of wire mark was proposed, based on the Fourier series expansion of the photodetector signal g(t).

Letting

$$g(t) = a_0 + \sum_{n=1}^{\infty} a_n \cos \frac{2n\pi t}{T} + \phi_n$$

the time-average or D.C. value of the signal g(t) would be equal to  $a_0$ , while the Fourier series component of the signal at any frequency  $f = \frac{2n\pi}{T}$  would be  $a_n$ . In particular, at the wire mark frequency where  $f = \frac{2\pi w}{T}$ , the Fourier series component would be  $a_w$ , and the wire mark index proposed was thus:

Wire Mark 
$$\stackrel{\Delta}{=} \frac{a_w}{a_o}$$

# 2.5 The Effect of the Average Fractional Area of Contact on the Proposed Wire Mark Index

It was pointed out by Dr. A.A. Robertson of the Institute staff that the above analysis indicating the ratio  $i_{f/I}$  to be independent of K, the average fractional area of contact of the paper with the prism, fails to take into account the variation of  $i_f$  due to the variation in contact waveform with changes in K.

This important question was attacked by considering the behaviour of the proposed wire mark index for a fictitious "ideally wire marked" sample in the Chapman Printing Smoothness Tester. It was assumed that the surface profile of the sample was purely sinusoidal at the wire mark frequency (Figure 3(a)), and that as the pressure applied to the sample was increased, the average fractional area of contact K could be increased from 0 to 100 per cent. The distribution of optical contact

along a given scanning line and the resultant photodetector signal g(t) for K = 50 per cent are given in Figures 3(b) and 3(c). (A true squarewave photodetector signal could be generated only by scanning the contact interface with an infinitely small light spot).

For the general case of Figure 3(d), where the photodetector signal has the value unity during the period of optical contact from 0 to  $\propto$ , and the value zero during the period of nonoptical contact from  $\propto$  to  $2\pi$ , the proposed wire mark index was found to have the value

$$W_{\bullet}M_{\bullet}(\propto) = \frac{2\sqrt{2}}{\propto} \sqrt{1 - \cos \infty}$$

This function is plotted in Figure 3(e). The proposed wire mark index is thus seen to be zero for continuous optical contact, rising to the value 4/11 for a square-wave contact distribution, and reaching the value 2 for very brief pulses of contact at the wire mark frequency. Since the behaviour of this function is in good agreement with physical intuition concerning the severity of wire marks, (i.e. smaller values are assigned to flatter surfaces), the definition of the wire mark index

W.M. = 
$$\frac{a}{a}$$
 was tentatively adopted.

#### 2.6 The Choice of a Scanning Waveform

In order to analyze the distribution of optical contact area over the paper surface by means of a frequency analysis of the photo-detector signal g(t), the generating light spot must scan over the contact interface at a constant velocity. In addition, information is also

desired about the contact area distribution in two specific directions: the machine and cross-machine directions of the paper. A rectangular scanning raster, formed either by sawtooth or triangular scanning waveforms, was thus dictated.

#### 2.6.1 Sawtooth Scanning Waveforms

The choice of a sawtooth scanning waveform presented two serious problems. The first of these is that retrace blanking of the light source between consecutive line scans and between frames, (in order to prevent very high frequency components from being introduced into the photodetector signal g(t) during the retrace periods), necessarily introduces negative pulses into g(t) at both the line and frame frequencies. Furthermore, because the instantaneous values of g(t) will rarely be the same at the end of one scan and the beginning of the next at a totally different position on the sample, both positive and negative going step functions are introduced into g(t) at both the line and frame scan rates. Harmonics of these pulses are certain to interfere with the frequency analysis of g(t), as they do in the Q.N.S/M. instrument. 2)

## 2.6.2 Triangular Scanning Waveforms

The alternative choice of triangular scanning waveforms offered a solution to both of the above problems, since no retrace blanking circuitry would then be required, and no extraneous pulses would be introduced into the filter circuitry. These two advantages were felt to outweigh by far the inherent difficulty of generating suitable triangular

wave sweep waveforms, and the latter choice of waveform was thus adopted.

## 2.7 The Problem of the Frequency Stability of the X-Axis Sweep Generator

One of the most important aspects of the design of the higher frequency sweep generator, (arbitrarily designated the X-axis sweep generator), was the problem of frequency stability.

On the assumption that

- a) there are m wire marks per inch;
- the X-axis sweep generator runs at x cycles per second,
   with two complete scans of the paper per cycle;
- c) the distance scanned at the paper surface in the X direction is d inches:

then the scanning speed v of the light spot over the paper surface will be given by v = 2xd inches per second, while the frequency  $f_w$  of the electrical signal corresponding to the wire mark will be given by  $f_w = mv = 2dmx$  cycles/second.

It was suggested that the desired wire mark range from m=10 per inch to m=100 per inch could be most easily covered by an electrical filter in the audio frequency range; say from  $f_{W}=1$  KC. to  $f_{W}=10$  KC. For an X-axis sweep width of d=1 inch, the X-axis sweep rate becomes

$$x = \frac{f_w}{2dm} = \frac{1000}{(2)(1)(10)} = 50$$
 cycles/second.

The problem of obtaining frequency stability in the X-axis sweep generator (which would be essential in order to calibrate the electrical filter in terms of spatial frequency at the paper surface)

could then be solved by synchronizing the X-axis sweep generator with the power line frequency of 60 cycles per second, and either tuning the filter over the range 1.2 to 12 KC., or reducing the X sweep amplitude to 0.866 inches.

The latter alternative, (although subsequently dictated in practice by the revamped optical system of the Wire Mark Meter), was not favoured for the following reason. The X sweep amplitude represents the longest uninterrupted distance scanned on the paper surface, and in order to perform a statistically significant frequency analysis, at least five periods of the lowest frequency being analyzed should be present in a single X sweep, ten periods being preferable.

## 2.8 The Limitation Imposed on the Size of the Scanning Light Spot

The limiting factor which arises at the high frequency end of the spectrum is the size of the generating light spot. Because no detail finer than the effective spot size can be resolved by the scanning technique, it was considered desirable to make the effective diameter of the light spot at the paper—to—glass interface no larger than 1/5 of the shortest wavelength being analyzed, i.e. not larger than 0.002 inches.

## 2.9 The Limitation Imposed on the Selectivity of the Filter Circuitry

Because the spatial resolution of the Q.N.S/M. Formation Tester was severely limited by the use of fixed 1/3 octave bandwidth electrical filters in the frequency analysis circuitry, it was felt that the corresponding filter circuitry of the Wire Mark Meter should be continuously

variable in frequency, and should have as high a Q as possible, consistent with reasonable analysis times.

It has been shown that the time required to perform a valid frequency analysis of a periodic signal with a uniform power spectrum depends only on the proportional standard error required and the bandwidth of the filter employed. <sup>6)</sup> If  $S_n$  represents the true power contained in a given harmonic of the signal g(t), and  $\mathcal{T}_n$  represents the r.m.s. error in the determination of that power, then the number of harmonics N in the passband of the filter required to obtain a proportional standard error  $\mathcal{T}_n/S_n$  will be  $\frac{1}{\sqrt{N}}$ . Thus for a proportional standard error of 5 per cent, there must be 400 harmonics in the passband of the filter, and using a filter with a Q of 20 at 5 KC. would require a record which is  $(\frac{400}{1} \times \frac{20}{5000}) = 8/5$  of a second long. A Q of 20 was accordingly proposed for the filter circuitry as a good compromise between high resolution and short analysis time. The corresponding analysis times required for the same proportional standard error at 1 KC. and 10 KC. are obviously 8 seconds and 4/5 of a second respectively for a filter with a Q of 20.

## 2.10 The Time Required to Completely Scan a Paper Sample

At this juncture, it was proposed that the low-frequency or Y-axis sweep should run at 3 cycles per second, with an amplitude of one inch at the paper surface. The resultant raster would then contain 20 lines per frame, and 6 frames per second, as shown in Figure 4.

It was decided not to synchronize the X and Y sweep generators, in order that the raster would not always sweep out the same pattern on

the paper surface. On the assumption that n complete X scans are performed during the time required for m complete X scans, (where m and n are integers), the scanning pattern will not repeat itself exactly until all m complete Y scans have occurred. If the X and Y scan rates are in the ratio of 20.001 to 1.000, a total of 5-1/2 minutes will elapse before the scanning pattern is repeated at a Y scan rate of 3 cycles per second. This superficial analysis however ignores the fact that two scans differing in position by less than one-half of the size of the scanning spot will be essentially identical. A more realistic upper bound for the time required to repeat a particular scan is given by the ratio of the height of the raster to one-half of the effective spot size. For a spot size of 0.002 inches, and a raster height of one inch, a total of about 1000 different scans are possible. At an X sweep rate of 60 cycles per second, a maximum of about 15 seconds would then be required before a given scan could be repeated.

#### 2.11 The Error in the Observed Wire Mark Frequency

As may be seen from the complete scanning raster depicted in Figure 4, the use of triangular sweep deflection waveforms means that the X sweep direction cannot be exactly parallel to either the machine or cross-machine directions of the paper sample being examined. As a consequence, the observed wire mark frequency  $f_w$  will always be lower than the true wire mark frequency  $f_w$ . If the ratio of X to Y sweep rates is as large as 20: 1 however; the observed wire mark frequency

$$f_{W}^{'} = \frac{f_{W}}{\sqrt{1 + 1/400}} \approx f_{W} (1 - 1/800)$$

will be essentially identical to f.

## 2.12 The Choice of a Scanning Method

In order to preserve a linear relationship between the distribution of optical contact over a given scanning line and the corresponding
photodetector signal, a somewhat stringent linearity tolerance of 1 per
cent was proposed for the X sweep waveform. Such a high linearity
requirement at a rate of 120 scans per second seemed to preclude the use
of mechanical scanning systems. It was therefore proposed to use a
flying spot cathode-ray tube as a scanning light source, and to image the
spot on the C.R. tube screen onto the paper-to-glass interface through
the compound prism of the Chapman Printing Smoothness Tester by means of
an intermediate lens. The proposed optical system is depicted in
Figure 5.

#### 2.13 The Choice of a Photodetector

Because the intensity of the spot on the C.R. tube screen would be low, it was expected that a photomultiplier tube would be necessary to detect the reflected light signal; and in order to achieve as high a luminous efficiency as possible, the photomultiplier and flying spot scanner tube were chosen as a matching pair. It was found that the Pl6 phosphor of the type 5ZPl6 flying-spot C.R.T. has the peak in its luminous output at a wavelength of 3825  $\Re$ ; so that the type 1P21 photomultiplier tube should be chosen, since the peak in its spectral sensitivity curve occurs in the region of 4000  $\Re$ .

## 2.14 The Proposed Block Diagram of the Wire Mark Meter

The complete block diagram proposed for the instrument is given in Figure 6.

## 2.14.1 Generation of the Scanning Raster

Generation of the scanning raster on the C.R. tube screen would require an electromagnetic deflection yoke, suitable X and Y sweep circuitry, and a well-regulated high voltage D.C. power supply to provide ultor and focusing electrode potentials for the C.R. tube.

## 2.14.2 Detection of the Reflected Light Signal

Conversion of the light signal at the paper-to-glass interface into an electrical signal g(t) would be accomplished by the photomulti-plier tube whose photocathode potential would be derived from a well-regulated high-voltage D.C. power supply.

## 2.14.3 Analysis of the Photodetector Signal

Analysis of the resultant signal g(t) would require three functional units: a D.C.-coupled video amplifier to preserve the full bandwidth of the P.M. tube signal while reducing its source impedance; a filtering amplifier with constant Q, constant gain, and variable frequency

to extract the Fourier series components of the signal g(t); and an averaging amplifier to take the D.C. value of either the video amplifier output, or the rectified output of the filtering amplifier.

# 2.14.4 Output Display

It was proposed initially to display the averaging amplifier output simply by means of a panel meter; with an auxiliary strip-chart recorder to be included later if its use for the plotting of surface roughness spectra were warranted.

## III : IMPLEMENTATION OF HARDWARE

## 3.1 Functions of the Electronic Systems of the Wire Mark Meter

As may be seen from the block diagram of the instrument given in Figure 6, the two primary functions of the electronics involved in the Wire Mark Meter are the generation of the raster on the screen of the flying-spot C.R. tube, and the subsequent analysis of the photomultiplier tube signal. In order to accomplish these functions, however, both control circuitry and various low and high voltage power supplies are necessary.

## 3.1.1 The P.M. Tube High Voltage Power Supply

Wherever possible, commercially obtainable units were purchased to perform specific functions in the instrument. For example, the photomultiplier tube high voltage power supply chosen was an N.J.E. Model S-325, which is capable of delivering from 500 to 2500 volts at 10 mÅ. with less than 5 mV. total ripple, noise and hum. In addition it provides a very stable output voltage, with an output drift of less than 0.1 per cent over an eight hour period. Remote turn-on of the high voltage output was the only modification necessary to this unit.

#### 3.1.2 The C.R. Tube High Voltage Power Supply

The C.R. tube high voltage power supply chosen was a Spellman Model RG30, providing a well-regulated D.C. output voltage of 15 to 30 KV.

at 1 mA. as a source of accelerating potential, and a low voltage output of 4 to 6 KV. for electrostatic focussing of the C.R. tube. Again, remote turn-on of the high voltage output was the only modification necessary.

#### 3.1.3 The C.R. Tube Deflection Yoke

The electromagnetic deflection yoke chosen was a Syntronic Instruments Type Y-16-A6P, which has a double push-pull configuration, and requires 100 mA. peak currents for half-screen-width deflection of a 5ZP16 operated at an accelerating potential of 22.5 KV.

## 3.1.4 Low Voltage Power Supplies

Low voltage power for both the sweep and analysis circuitry is drawn from three low voltage power supplies, a Lambda Model C282 giving +450 volts at 200 mA., and two Model C281 Lambda units delivering ± 250 volts at 200 mA.

#### 3.2 The Scan Generation Circuitry of the Wire Mark Meter

Because of the high cost of commercially available triangular wave function generators, it was decided to attempt construction of these units; especially since the X sweep oscillator would be line synchronized, and the Y sweep oscillator would have to be tuned only over the narrow frequency range of about 1 cps to 6 cps. The choice of such a low Y sweep frequency obviously dictated that the Y sweep circuitry would have to be D.C.—coupled throughout, and it was accordingly decided to make the X sweep circuitry D.C.—coupled as well in the interests of interchangeability

and economy of design. Thus two completely independent D.C.-coupled 50 watt push-pull power amplifiers were required.

## 3.2.1 The Generation of Triangular Wave Sweep Waveforms

The choice of a balanced push-pull deflection yoke, while eliminating the problems associated with single-ended output circuitry, introduces the alternative problem of generating two complementary wave-forms with which to drive the output stages. Two complementary triangular waveforms could be generated simultaneously by integrating two complementary square wave signals, either by means of RC networks directly, or by means of operational amplifiers as integrators. The latter method was ruled out as impractical however, since it would be required that the square wave signals have zero mean value, in order that the time integral of the square wave not increase or decrease indefinitely.

#### 3.2.2 The Generation of Complementary Square Wave Signals

Two complementary 60 cycle square wave signals could be obtained, it was reasoned, from the plate and cathode of a triode phase inverter stage, while the input to the phase inverter could be obtained by suitably amplifying and clipping the 60 cycle line voltage. Appropriate 3 cps square wave signals could likewise be obtained from a phase inverter stage, but the problem then arose of finding a 3 cps sine wave oscillator. It was felt that a more satisfactory solution to the whole problem would be to construct similar 60 cps and 3 cps triggering oscillators with which to drive identical bistable D.C.—coupled multi-

vibrators. The plate voltage waveforms of the multivibrators then would be the required complementary square waves.

#### 3.2.3 The Choice of Triggering Oscillator

The initial design of the sweep generator section utilized 2D21 gas thyratrons as relaxation oscillators for triggering purposes, but they were found to be very unstable with time, drifting continuously in frequency as they warmed up. Although the 60 cycle oscillator could be periodically returned to line synchronization, the low frequency oscillator could not always be reset; and since the Y sweep amplitude of the raster on the C.R. tube screen was inversely proportional to the Y sweep oscillator frequency, it was finally found necessary to replace the gas thyratron relaxation oscillators with triode blocking oscillators. (In order to have multivibrator output frequencies of 60 cps and 3 cps, the actual frequencies of oscillation of the high and low frequency oscillators have to be 120 cps and 6 cps respectively). The complete circuitry for both types of oscillator are given in Appendix I: Figure A.

The overall block diagram of the X and Y sweep circuitry is given in Figure 7. The detailed circuitry of the multivibrator-integrator section will be found in Appendix I: Figure B; while the detailed X and Y sweep power amplifier circuitry appears in Appendix I: Figure C.

#### 3.2.4 The Correspondence Between Actual and Desired Sweep Waveforms

The two square wave signals at the plates of the multivibrator have a peak-to-peak amplitude of 150 volts, and are connected to two

identical R-C networks to ground. (Figure 7) The effective value of R is determined by the parallel resistance of  $R_1$ ,  $R_2$ , and  $R_3$ , so that the R-C time constant  $\mathcal{T}$  of the network is thus

$$\mathcal{T} = \frac{R_1 R_2 R_3 C}{(R_1 R_2) + (R_2 R_3) + (R_1 R_3)}$$

The actual sweep waveform  $F_a(t)$  at the point P in Figure 7 is a series of positive and negative-going exponentials superimposed on an average D.C. level, as shown in Figure 8(b). The equation of  $F_a(t)$  is given by

$$F_{a}(t) = -5 + \left\{ 75 \left[ (1 - e^{-\frac{t}{5}}) \right] - 150 \left[ (1 - e^{-\frac{t}{5}}) \right] \left[ u_{o}(t - T) \right] + 150 \left[ (1 - e^{-\frac{t}{5}}) \right] \left[ u_{o}(t - 2T) \right] - + - + \cdots \right\}$$

$$= -5 + 75 \left\{ \left[ 1 - e^{-\frac{t}{5}} \right] - 2 \left[ 1 - e^{-\frac{t}{5}} \right] \left[ u_{o}(t - T) \right] + 2 \left[ 1 - e^{-\frac{t}{5}} \right] \left[ u_{o}(t - 2T) \right] - + \cdots \right\}$$

$$\approx -5 + 75 \left\{ \left[ \frac{t}{5} - (\frac{t}{2}) \left( \frac{t}{5} \right)^{2} - 2 \left[ \frac{t}{5} - (\frac{t}{2}) \left( \frac{t}{5} - T \right)^{2} \right] \left[ u_{o}(t - T) \right] + - \right\}$$

where  $u_{o}(t-T)$  represents a unit step function beginning at the time t = T.

The desired waveform  $F_d(t)$  is depicted in Figure 8(c), and its equation is given by

$$F_{d}(t) = -5 + 5 \left\{ \left[ \frac{t}{T} \right] - 2 \left[ \frac{t-T}{T} \right] \left[ u_{o}(t-T) \right] + 2 \left[ \frac{t-2T}{T} \right] \left[ u_{o}(t-2T) \right] + - + - \left( - \right)^{n} 2 \left[ \frac{t-nT}{T} \right] \left[ u_{o}(t-nT) \right] \right\}$$

In order to make the actual and desired waveforms agree as closely as possible, it is only necessary to make the R-C time constant  $\mathcal{T}$  of such a value that  $\frac{75}{\mathcal{T}} = \frac{5}{1}$  i.e. such that  $\mathcal{T} = 151$ .

The difference between the two curves will be given by the second order term  $1/2(t/T)^2$ , and will have a value of only 1/450 when T = 15T, which is well within the desired linearity tolerance of one per cent.

#### 3.2.5 Linearization of the Output Current Waveforms

Having thus obtained two complementary triangular wave signals of suitable amplitude and with the desired linearity, it was then only necessary to ensure that the magnetic deflection yoke current waveforms were made linearly proportional to the input voltage waveforms. This step was accomplished by means of two identical inverting operational amplifiers which were used to drive the input grids of two type 6550 beam power pentodes. The push-pull deflection yoke was connected between the 6550 plate leads and the +450 volt low voltage power supply, while current

feedback signals to close the loops around the operational amplifiers were obtained from adjustable resistors in the 6550 cathode returns to ground. Fixed resistors in the cathode leads provide convenient test points for monitoring the total cathode current.

# 3.2.6 Fail-Safe Design Features Incorporated into the Sweep Circuitry

In order to protect the output pentodes from current overloads due to the failure of the triggering oscillator, multivibrator or operational amplifiers, 150 mA. fuses were placed in the 6550 cathode leads.

Because quite some time is required for the D.C. voltages at point P of Figure 7 to come to their steady-stage values after the instrument is first switched on, no D.C. voltages are applied to the operational amplifiers until the sweep generators have been running for several minutes. In addition, shunt diode limiters were placed at the operational amplifier inputs to clamp their input signals at about -11 volts in the event of failure of the sweep generating circuitry. (This feature was proven invaluable during the period when tempermental gas thyratrons were used as sweep oscillators).

# 3.2.7 Adjustment of the Peak and Average Values of the Deflection Currents

The peak amplitude of the deflection currents may obviously be set by means of the variable cathode resistors in the output stage, while the position of the raster on the C.R.T. screen is determined by adjusting the average D.C. level of the input voltages to the operational amplifiers at point P.

## 3.3 Control Circuitry of the Wire Mark Meter

In order to protect the flying-spot C.R. tube from the application of accelerating potential in the absence of deflection currents in the yoke, or control grid bias, somewhat elaborate control circuitry was designed to perform the following functions:

- a) apply ± 250 volt potentials to the blocking oscillators and multivibrators of the sweep circuitry, and to the operational amplifiers of the analysis circuitry during the WARMUP mode.
- b) apply ± 250 volt potentials simultaneously to the operational amplifiers and screen grids of the 6550 power amplifiers during the STANDBY mode, enabling the sweep circuitry to be adjusted.
- c) apply accelerating potential to the C.R. tube, and high voltage to the P.M. tube during the ON mode.

It was further desired that transfer to the ON mode from the STANDBY mode could be performed only if the following criteria were met:

- a) all three low voltage power supplies were at least 80 per cent of their nominal value.
- b) the lead supplying control grid bias to the C.R. tube was connected to the C.R. tube enclosure.

c) the cable connecting the deflection yoke to the sweep circuit power amplifier was properly plugged in.

Furthermore, if any of the three low voltage power supplies were to fail during normal operation, the instrument was to return automatically to the WARMUP mode.

The complete circuit diagram of the control circuitry devised to fulfil the above requirements is given in Appendix I: Figure D.

## 3.4 Protective and Safety Circuitry of the Wire Mark Meter

A low reverse-leakage semiconductor diode and a large storage capacitor were used to make the time constant of the C.R. tube control grid bias much longer than the time constant of the accelerating potential power supply, in order to protect the C.R. tube in the event of power line voltage failure.

An electrical interlock on the C.R. tube enclosure prevents the application of accelerating potential with the C.R. tube exposed, while a similar switch on the inspection port cover of the Chapman Printing Smoothness Tester turns off the P.M. tube power supply before room light is admitted to the photomultiplier tube housing.

## 3.5 The Analysis Circuitry of the Wire Mark Meter

A photograph of the complete Wire Mark Meter is given in Figure 9. On the left is the modified Chapman Printing Smoothness Tester, surmounted by the C.R. tube enclosure; while on the right is the main cabinet containing the control, sweep, and analysis circuitry.

#### 3.5.1 Connection to the Photomultiplier Tube

Because the photomultiplier tube and analysis circuitry were necessarily several feet apart, careful consideration had to be given to the problem of connecting the P.M. tube to the video amplifier. Because the photomultiplier tube behaves as a very weak (1 uA.) current source, careful shielding of the anode lead is necessary, but then the shunt capacitance  $C_s$  of the shielded cable has an adverse effect on the available bandwidth of the P.M. tube signal. One solution to the problem would be to place a simple cathode-follower stage close to the P.M. tube in its light-tight enclosure, but then the D.C. level of the video signal would be lost. The problem was solved by designing the video amplifier with an input cathode-follower stage, and connecting the shield of the P.M. tube lead to the cathode-follower cathode. If the gain of the input cathode follower stage is G, then the effective shunt capacitance  $C_{\mathbf{f}}$  of the input lead may be reduced by a factor of (1-G). Assuming a source impedance for the P.M. tube of  $R = 10^6$  ohms, a shunt cable capacitance  $C_{\rm s}$  of 100 pf, and a cathode follower gain G of 0.9, the half power bandwidth  $f_{1/2}$  of the input circuit will be given by

$$f_{1/2} \approx \frac{1}{2\pi RC_f} \approx \frac{1}{2\pi R(1-G)C_s} = \frac{50}{\pi} K.C.$$

(This value was later confirmed experimentally by observing the video amplifier output while applying Z-axis modulation to the C.R. tube with a variable frequency audio generator.)

#### 3.5.2 The Video Amplifier

As may be seen from the detailed circuit of Appendix I:
Figure E, the video amplifier consists of a high-gain D.C.-coupled operational amplifier with extended frequency response. 7) Full negative feedback was applied through a one megohm resistor, so that the video amplifier output is thus one volt per microampere of P.M. tube anode current. The bandwidth of the amplifier above was experimentally verified as greater than 100 KC.; well beyond the highest frequencies present in the video signal. Drift of the D.C. output level is corrected by means of a small variable bias voltage applied to the differential input grid of the input stage.

#### 3.5.3 The Averaging Amplifier

Determination of the average D.C. level of the output of the video amplifier and the rectified output of the filtering amplifier is accomplished by the averaging amplifier, which uses the same basic operational amplifier circuit as in the video amplifier, but with its input and feedback impedances such that the overall amplifier behaves as a low-pass filter of variable cutoff-frequency, and with a D.C. gain variable between 10 and 50 times. Having an adjustable cutoff-frequency allows the operator to choose a suitable time constant for damping the output panel meter, which is connected directly across the amplifier output. As in the case of the video amplifier, long term drift may be corrected by means of bias applied to the differential input terminal.

## 3.5.4 The Filtering Amplifier

The most ambitious aspect of this project was undoubtedly the development of a suitable filtering amplifier to extract the Fourier series component of the video signal. Although it was definitely felt that the Q and gain of the filtering amplifier should both be independent of frequency over the range of 1 KC. to 10 KC., it was by no means certain whether or not a Q of 20 would be the optimum value. In view of the limited frequency range requirement, and the uncertainty of the Q requirement, it was decided to attempt construction of suitable filtering circuitry using an operational amplifier in conjunction with a Twin-T feedback network.

The null frequency  $f_o$  of the unloaded Twin-T network, whose elements are R, R, R/2; C, C, 2C (Figure 10(a)), is given by  $f_o = \frac{1}{2\pi RC}$ .

At this frequency, the magnitude of the transfer function of the network is a minimum, and it may be shown that by connecting the network as in Figure 10(b), a frequency selective amplifier is formed whose overall gain G is given by

$$G = \frac{e_0}{e_i} = \frac{-A_1 \left[1 - j\left(\frac{4}{\omega/\omega_0 - \omega_0/\omega}\right)\right]}{\left[1 - A_2 - j\left(\frac{4}{\omega/\omega_0 - \omega_0/\omega}\right)\right]}$$

The effective Q of this amplifier may then be shown to be

$$Q_{eff} = \left[ \frac{1}{\omega_{1,2}/\omega_{0} - \omega_{2}/\omega_{1,2}} \right] \approx \left[ \frac{1 - A_{2}}{4} \right], A_{2} > 10$$

A frequency selective amplifier was thus proposed using the circuit of Figure 10(c), where in the overall gain  $G = {}^{-R}o/R_1$  and the effective  $Q \approx \frac{R_0}{4R_f}$  could be adjusted independently.

It was soon found, however, that correct loading of the Twin-T network is extremely important for feedback amplifier applications. 8) The simplified analysis given above fails to take into account both the loading effect of the Twin-T network on an amplifier with finite output impedance, and the effect of loading of the Twin-T network itself by the feedback resistor  $R_f$ . The input impedance of the unloaded Twin-T network at its null frequency is given by  $Z_{in} = \begin{bmatrix} R/2 \\ -1 \end{bmatrix}$ , and is inversely proportional to the null frequency. In order to prevent the variation in input impedance of the Twin-T network with frequency from changing the overall gain G of the amplifier, it was found necessary to drive the Twin-T network with a high-transconductance cathode-follower stage. Variations in the bandwidth of the Twin-T network with frequency due to the loading effect of the feedback resistor  $R_f$  were also alleviated by interposing a cathode-follower stage between the Twin-T network and  $R_f$ .

Extremely close matching of the elements of the Twin-T network was found necessary. The capacitive elements were formed by silver-mica capacitors padded to 0.1 per cent tolerance. The resistive elements

were formed by deposited carbon resistors selected to a tolerance of 0.1 per cent; and connected in series with three ganged precision wire-wound potentiometers. In actual fact, it turned out that the practical upper limit to the effect Q of the filter amplifier was determined by the mechanical backlash and tracking error of the wire-wound potentiometers.

By means of switched capacitors in the Twin-T network, the amplifier may be tuned over two ranges 0.6 to 2.4 KC. and 2.4 to 9.6 KC. With the effective Q fixed at about 20, the gain of the amplifier is constant to within ± 3 per cent of the gain at 5.0 KC over both the high and low frequency ranges. The complete circuit diagram of the filtering amplifier is given in Appendix I: Figure F.

Half-wave rectification of the filter amplifier output is provided by a low reverse-leakage semiconductor diode with a resistive load.

# 3.5.5 Operation of the Analysis Circuitry

A diagram showing the interconnection of the various units of the analysis circuitry is given in Appendix I: Figure G. The main FUNCTION switch, Sl, has the following six positions, starting from the position indicated.

a) METER ZERO - The input of the averaging amplifier is grounded and the averaging amplifier bias circuit adjusted to give zero output on the panel meter.

- b) VIDEO ZERO The video amplifier input is left opencircuited with its output connected to the averaging amplifier input, and the video amplifier bias adjusted to give zero output on the panel meter.
- c) CALIBRATE METER The video amplifier input is connected to an external calibrating circuit with a known D.C. output and a known 5 KC. A.C. output. The gain of the averaging amplifier is adjusted to make the output meter read full-scale.
- d) CALLERATE FILTER The filter amplifier is tuned to 5.0 KC.

  and interposed between the video amplifier output and the

  averaging amplifier input. The gain of the filter amplifier

  is adjusted so that the output meter reads full-scale.
- e) READ VIDEO The input of the video amplifier is connected directly to the photomultiplier tube anode, and the P.M. tube high voltage power supply is adjusted such that the average D.C. level of the video signal drives the output meter to full-scale.
- f) READ FILTER The filtering amplifier is again interposed between the video and averaging amplifiers, and the panel meter reads the filter output directly. A surface roughness spectrogram may then be taken by tuning the filter amplifier with the built-in synchronous motor while simultaneously recording the averaging amplifier output.

In addition, in order to prevent stray pickup, the FUNCTION switch grounds the external calibrator input in positions a, b, e, f; and the filtering amplifier input in positions a, b, c, e.

A shunt resistance of 22 megohms to ground is kept on the photomultiplier tube anode lead in order that it will not be left open-circuited.

# 3.5.6 External Calibrating Circuitry

Because the accuracy to which the components of the video signal may be determined is governed directly by the accuracy of the test signal used to calibrate the analysis circuitry, a special external calibrating source was built. The external calibration source may in turn be rapidly checked at any time for the accuracy of the ratio of its A.C. to D.C. outputs by means of an oscilloscope. The precision of this setting of the calibrating circuit is better than 0.1 per cent, and is independent of the oscilloscope calibration. The circuit diagram of this external calibrator is given in Appendix I: Figure H.

#### IV : GENERAL DISCUSSION

#### 4.1 The Lack of Resolution in the Initial Results

Early attempts to measure wire mark with the instrument were not at all promising: initial surface roughness spectra taken on heavily wire-marked papers over the range of 30 to 90 marks per inch revealed only a very small component at the expected wire mark frequency. No component attributable to wire mark could be found at all in the surface roughness spectra of lightly wire-marked samples.

It was also found that the time-average value of the video signal from the near and far sides of the paper sample differed by a factor of almost three-to-one. When this variation occurred at the low frequency (Y scan) rate, it became necessary to heavily overdamp the output panel meter in order to estimate the time-average value of the averaging amplifier output. As a consequence, about fifteen seconds were required to take a single output reading, and about ten minutes to plot a single surface roughness spectrum.

The comparison of about a dozen such surface roughness spectra however, revealed one most significant fact: in addition to the lack of wire mark peak, all the spectra decreased uniformly in amplitude from the low to the high frequency end. Since it was expected that the high frequency components of the video signal would be at least as strong as the low frequency components, it became apparent that the overall system was also suffering from a serious lack of resolution.

# 4.1.1 Measurement of the Bandwidth of the Photodetection System

In attempting to find the causes of this lack of resolution, the first step taken was to measure the electrical bandwidth of the photomultiplier-video amplifier combination. This was done by placing an oiled sheet of opal glass in place of the paper sample in the Chapman Smoothness Tester, while applying Z-axis modulation to the C.R. tube. The half-power bandwidth of the system was then found to be just below 20 KC., as expected. It was also found that the intensity modulation of the C.R. tube with a square wave signal of a given frequency increased the filtering amplifier output by a factor of about 1.25 with respect to sine wave modulation of the same peak-to-peak amplitude. This result compared favourably with the expected increase of 4/11 predicted by theory.

## 4.1.2 Measurement of the Effective Spot Size of the Scanning Light Spot

The second step taken in the search for the factors limiting the resolution of the instrument was a measurement of the effective size of the scanning light spot at the paper—to—glass contact interface. This was done by means of the edge—sweep test, which is performed by repeatedly scanning the light spot over a narrow dark bar of known width, and by comparing the time required for the resultant video signal to fall to 1/e of its initial value to the time required for the spot to traverse the dark band. 9) (The method suffers from a lack of precision, but gives an estimate of the effective spot size to within about ten per cent).

Such measurements indicated that the effective spot size at the paper-to-glass interface was about 0.02 inches, rather than the desired value of about 0.002 inches.

By means of the same edge-sweep test it was then determined that the effective spot size at the C.R. tube screen was less than 0.01 inches, which implied that although the optical system reduced the overall raster by a factor of 2.3, yet it increased the size of the scanning light spot by a factor of more than two.

# 4.2 Improvements in the Optical System

The optical system of the instrument was accordingly rebuilt, using an 80 mm. focal length f2.8 coated anastigmat lens in place of the simple lens used previously. The overall demagnification of the new optical system was measured as 3.3:1, while the resultant spot size at the paper-to-glass interface was reduced to less than 0.006 inches when both the optical lens and C.R. tube were critically focussed. Although not meeting the design criterion of 0.002 inches, this value of spot size was considered just acceptable.

At the same time it was discovered that the three-to-one variation found in the video signal amplitude from one side of the sample to the other was attributable partly to the difference in optical paths between the two sides of the sample and the photomultiplier tube, and partly to misalignment of the photomultiplier tube with respect to the prism. With careful alignment of the P.M. tube, the average video signal amplitude from one side of the sample to the other could be kept within

the range of about three-to-two. It was further realized that by keeping the high frequency scanning direction across the width of the sample, the unavoidable variations in video signal level due to optical path differences would occur at 60 cps, rather than at 3 cps. As a consequence, much less damping of the output panel meter was necessary, and complete surface roughness spectra could then be taken much more rapidly.

#### 4.2.1 Disadvantages of the Rebuilt Optical System

The revamped optical system was not without its attendant draw-backs, however. Because the largest raster which could be generated on the face of the five inch diameter flying spot C.R. tube was only three inches square, the high demagnification of the focusing lens limited the maximum size of the raster on the sample to about 0.9 inches square. The design criterion of a one inch square sample area was thus no longer met. In addition, by fixing the orientation of the scanning raster with respect to the prism, the design criterion of measuring both the machine direction and cross-machine direction spectra on the same sample became attainable only by releasing the hydraulic pressure applied to the backing plate and physically rotating the sample through ninety degrees. This latter procedure was more time consuming and considerably less desirable than simply rotating the electromagnetic deflection yoke around the neck of the flying-spot C.R. tube.

#### 4.3 Improvements in the X and Y Sweep Circuitry

It was at this juncture that the decision was made to eliminate the gas thyratron relaxation oscillators of the X and Y sweep circuitry. Several hundred hours of operation had proven that they were extremely temperature sensitive, drifting badly in frequency as they warmed up, or sometimes completely ceasing to oscillate. Because a failure of the X sweep oscillator left only a very slowly moving spot on the C.R. tube screen, whereas failure of the Y sweep oscillator left a rapidly moving spot, the X sweep oscillator was changed first to the triode blocking oscillator described earlier. The same circuit was subsequently easily adapted to the lower frequency of the Y sweep oscillator. Both blocking oscillator circuits have since proven themselves to be very reliable and stable with respect to temperature.

# 4.4 The Problems of Thermal Drift

Thermal drift, however, remains a problem in several other areas of the instrument, particularly in the D.C.—coupled multivibrator stages immediately following the X and Y sweep blocking oscillators. Both multivibrator anode waveforms are square waves whose upper value (about +225 volts) is relatively stable, but whose lower value (about +75 volts) is subject to considerable thermal drift. This disparity of behaviour occurs because the higher anode voltage level occurring during cut-off of one triode section is determined solely by the resistive voltage divider connected to the anode lead, whereas the lower anode voltage level is essentially determined by the plate current which flows when the triode

is turned full on. This latter current is heavily influenced by the emission of the tube, which in turn is quite sensitive to the operating temperature. The lower anode voltage level then drifts downward continuously as the sweep circuit power amplifier chassis warms up.

The D.C. levels of the input voltages applied to the following operational amplifier stages however, are necessarily related to the average D.C. levels of the multivibrator anode voltages, with the result that the average D.C. levels of the currents flowing in the deflection yoke drift steadily upward as the instrument warms up. In order to prevent excessive plate current in the sweep circuit power output stages, it is thus necessary to monitor the output power pentode plate currents continuously during warmup of the instrument.

Some thermal drift also occurs in the outputs of the video and averaging amplifiers, but the total drift voltages during a one hour period after warmup represent less than five per cent of the full scale output of the instrument, and these are easily corrected by means of the appropriate bias controls.

# 4.5 The Faults in the Filtering Amplifier Circuitry

Because the filtering amplifier is A.C.-coupled, no correction for its output drift is required. It does have however, several other faults. Foremost among these is the lack of reproducibility among the settings of the three sections of the three-gang wire-wound potentiometer which forms the variable element of the Twin-T filter network. Mechanical backlash, rather than disagreement between the separate resistance-versus-

rotation curves, would seem to be the problem here.

A second serious fault in the filtering amplifier lies in the nonlinearity of the transfer characteristics of the semiconductor output rectifier. Appreciable nonlinearity is apparent for output meter readings in the lowest 10 per cent of the scale, so that it is necessary to change the gain of the filtering amplifier by a factor of three to keep the output meter reading in the upper half of the scale.

#### 4.6 Capabilities of the Completed Instrument

In spite of the drawbacks detailed above, the completed instrument nonetheless meets the majority of its design objectives. Specifically:

- a) the instrument is capable of measuring wire mark over the spatial frequency range of 1/6 to 1/90 of an inch, and can clearly differentiate between machine direction and cross-machine wire marks.
- b) the method is applicable to both opaque and coated paper samples, and does not include printing of the paper as part of the measurement procedure.
- c) the measurement is made over an area of approximately one half of a square inch while the sample is subjected to pressures typical of those encountered in the printing process.

#### V : EXPERIMENTAL RESULTS

Although wire mark represents a continuing problem in the wireside printing of many grades of paper, the measurement of wire mark and the subsequent alleviation of the wire mark problem will be of the greatest significance to the newsprint industry. For this reason, by far the most work done with the Wire Mark Meter to date has been on newsprint paper grades.

# 5.1 Typical Surface Roughness Spectra of Newsprint

Surface roughness spectra (i.e. plots of the distribution of contact area vs. spatial frequency) have been taken on a wide variety of newsprint samples as part of a comprehensive study of the wire mark problem in Canadian newsprint. 10)

From the wide selection of samples obtained for the above program, particular specimens from different paper mills which displayed strong, average, and weak wire marks were chosen by the author. Surface roughness spectra were then taken on both the top and wire sides of the sheets, and in both the machine and cross-machine directions. To facilitate intercomparison among the spectra, all samples were subjected to the same prism pressure of 300 psi, and all spectra were recorded to the same scale. The machine direction spectra (both top and wire side) are depicted in Figures 11, 13, and 15 for the samples displaying strong, average, and weak wire marks respectively; while the corresponding cross-

machine direction spectra are given in Figures 12, 14, and 16.

# 5.1.1 Characteristics of Top Side Spectra

The first observation which may be made from these curves is that the top side spectra lie close to, but in general below, that of the corresponding wire side curves. In addition, the top side spectra are relatively flat, displaying no pronounced peaks.

## 5.1.2 Characteristics of Wire Side Spectra

The wire side spectra on the other hand, all display peaks. In the case of the machine direction curves, these peaks are seen to occur in the region of 50 marks per inch, whereas in the case of the cross-machine direction curves, peaks occur in the regions of 65 and 45 marks per inch. In addition, the wire side machine direction spectra of news-print often exhibit a small peak in the neighbourhood of 17 marks per inch, as may be seen in Figure 11.

The spatial frequencies of all these peaks may be directly related to the structure of the Fourdrinier wires upon which these papers were made. One of the most common types of Fourdrinier wire used in the newsprint industry is a twill-woven wire with a mesh count of 68 x 52, i.e. having 68 strands per inch in the cross-machine direction and 52 strands per inch in the machine direction. The peaks in the cross-machine direction spectra near 70 marks per inch, and the peaks in the machine direction spectra near 50 marks per inch thus correspond directly to the fundamental mesh count of the Fourdrinier wire. Less apparent is the

origin of the cross-machine direction peaks near 45 marks per inch and the machine direction peaks near 17 marks per inch. These frequencies, however, are seen to be 2/3 and 1/3 respectively of the fundamental cross-machine direction and machine direction frequencies; and they are therefore also directly related to the mesh count of the Fourdrinier wire upon which the paper was initially formed. It has been found in general that the 2/3 subharmonic of the cross-machine direction peak has almost as great an amplitude as the fundamental, whereas the 1/3 subharmonic of the machine direction peak is usually very weak, or absent entirely. These observations are attributed to the nature of the twill weave pattern used in the weaving of Fourdrinier wires.

The magnitude of the fundamental wire mark peaks is seen to vary considerably among various commercial newsprint samples. As an example, the machine and cross-machine direction wire mark peaks for the strongly wire-marked sample (Figures 11 and 12) are 13.7 per cent and 8.8 per cent; whereas the corresponding peak heights for the weakly wire-marked sample (Figures 15 and 16) are only 6.6 per cent and 7.2 per cent respectively.

The direct comparison of peak heights in the above manner, however, fails to take into account the "random noise" component of the spectra, the magnitude of which reflects the overall roughness of the paper surface. Much greater variations are found to exist between individual samples when the difference between the peak heights and the average levels to be expected in the absence of a wire mark peak are compared. For want of a better name, these differences have been called

the "excess height" differences, and are illustrated in Figure 17. As an example, the "excess height" differences in the case of the strongly wire-marked sample (Figures 10 and 11) are 8.7 per cent and 2.2 per cent in the machine and cross-machine directions, whereas the corresponding differences for the weakly wire-marked sample (Figures 15 and 16) are only 1.6 per cent and 1.5 per cent.

#### 5.2 The Choice of a Wire Mark Index

Two possible indices for the quantitative assessment of wire mark thus present themselves: the peak height of the curve, h<sub>max</sub>; and the excess height, △h. The question then arises as to which of these two possible criteria would be a better measure of wire mark. In addition, should both machine direction and cross-machine direction wire mark readings be combined into a single wire mark index; and if so, in what manner?

One way of answering these questions would be to compare the peak height and excess height readings derived from the Wire Mark Meter for a given series of samples with readings on the same samples taken by an independent instrument already known to be capable of assessing wire mark. Unfortunately, no such independent instrument is known to exist.

# 5.2.1 The Correlation of Wire Mark Meter Readings With Visual Grading

Because wire mark does not actually manifest itself as a problem until the final printing of paper, it is often regarded as a paper printability problem. It is not surprising, therefore, that wire mark is

commonly assessed by the subjective method of the visual grading of printed samples; i.e. the intensity of wire mark on a given sample is evaluated by comparing it with a wide selection of standard samples bearing wire marks of different intensities.

It was accordingly proposed to assess the suitability of the Wire Mark Meter as an instrument for the objective determination of wire mark by means of a controlled experiment in which the Wire Mark Meter ranking of a series of unprinted newsprint samples was to be compared with the subjective ranking of an identical series of printed samples by a panel of competent judges. In order for this to be a valid comparison, the following conditions were deemed necessary:

- a) the selection of newsprint samples had to cover the range between heavily wire-marked and lightly wire-marked in a fairly uniform manner;
- b) the printed samples had to be essentially identical to their unprinted counterparts, and all had to be printed in an identical manner;
- c) the panel of judges had to be competent, unbiased, and not influenced in their judgement of wire mark by extraneous factors such as the brightness or formation of the samples.

A total of twenty different newsprint samples covering the complete range of commercial Canadian newsprints from heavily wire-marked to lightly wire-marked was thus examined in the Wire Mark Meter, under the supervision of Mr. T.S. Duchnicki. Complete spectra were taken in

the machine and cross-machine directions, and the heights of all peaks and the corresponding background levels read off and recorded. An identical set of samples was then printed by the NPIRI wedge method 11) on the Institute Vandercook proof printing press, and the resulting prints ranked in order of increasing wire mark by a panel of three independent judges, of which the author was a member.

Correlations were then sought by Mr. Duchnicki between the average subjective ranking of the printed samples and various possible wire mark indices derived from the Wire Mark Meter readings on unprinted samples. The strongest correlations were found to occur when the sum of the machine direction and cross-machine direction measurements was used; while it appeared that the simple peak height of the curve at the wire mark frequency was somewhat better as a wire mark index than the excess height index.

Proposed Wire Mark Index	Rank Correlation Coefficient	
Peak Height - h max	0.75	
Excess Height - $\triangle$ h	0.65	

Neither of these correlation coefficients was deemed by the judges to be remarkably good, and a close examination was therefore made of all the samples involved in the test. It was found that in several cases a wide disparity existed between the Wire Mark Meter ranking and the subjective ranking of similar samples, and that this disparity could be attributed to a tendency of the judges to be influenced by the large

scale formation defects in the samples. Accordingly, a second set of samples was printed, but in this latter case, the heavily-inked portions were blanked off before being ranked by the judges. Considerable changes were evidenced in the ranking of particular samples, while the rank correlation coefficients were found to increase accordingly.

Proposed Wire Mark Index	Rank Correlation	
<del> </del>	Coefficient	
h <sub>max</sub>	•93	
△ h	•92	

On the basis of these results, both of the proposed wire mark indices would appear to be equally good. From a study of the wire mark intensity on experimental pressure-formed handsheets however,  $^{10}$  it would appear that because the excess height index  $\triangle h$  takes into account the difference between the periodic and random surface roughness variations, it is to be preferred somewhat over the peak height index  $h_{max}$ .

The author is indebted to Mr. T.S. Duchnicki for permission to report the above results.

## 5.2.2 Theoretical Considerations in the Choice of a Wire Mark Index

The above observations lead naturally to a discussion of the fundamental problem of analyzing the photodetector signal g(t). It will be remembered that the method of analysis which was initially proposed and subsequently followed was to take as an index of wire mark intensity the ratio of the time-average value of the rectified filtered component

of g(t) to the time-average value of g(t). This procedure in effect yields the relative amplitude spectrum of g(t).

A more conventional approach, certainly as far as the communications engineer is concerned, would have been to take as an index of wire mark intensity the ratio of the time-average value of the squared filtered component of g(t) to the time-average value of g(t) squared. This latter procedure would in fact yield the relative power spectrum of g(t); that is to say, it would reveal the way in which the power available in g(t) is distributed with frequency. If, indeed, it is desirable to distinguish between the random and periodic components of surface roughness, (as the results of experiments with pressure-formed handsheets would seem to indicate), then the following technique could be used:

- a) From the plot of the relative power spectrum of g(t) determine the power in the wire mark components at various frequencies in the machine and cross-machine directions as  $S_1$ ,  $S_2$ ,  $S_3$ , etc.
- b) Determine the corresponding values of the random noise levels near the above wire mark frequencies as N<sub>1</sub>, N<sub>2</sub>, N<sub>3</sub>, etc.
- c) Take as an index of wire mark the sum of the power of the individual wire mark peaks minus the sum of the power of the adjacent random noise levels.

$$W.M. = \sum_{n=1}^{\infty} s_n - \sum_{n=1}^{\infty} N_n$$

Such an index would obviously be zero for a uniform spectrum of random noise, and would indicate directly the relative power in the wire mark components of g(t).

The question immediately arises however, as to how the power in the wire mark components of g(t) would be related to the way in which the printability of paper is affected by wire mark. The following points should be considered:

a) The conversion from the surface profile of a paper sample to optical contact is highly nonlinear. The loss of optical contact occurs at paper-to-prism separations of the order of one quarter of the wavelength of the light used, roughly 0.1 microns. Typical ink film thicknesses, however, are in the range of 5 microns, while the depressions in a paper surface may be as large as 25 microns or more. Thus, although the photodetector signal g(t) may be a linear function of the distribution of optical contact between a paper sample and the prism of the Chapman Printing Smoothness Tester, it will certainly not be a linear function of the surface profile of the paper sample. Furthermore, since g(t) carries no information about depressions in a paper surface deeper than about 0.1 microns, there could exist an infinite number of different paper surfaces all of which would give the same photodetector signal g(t). This observation is probably the most serious theoretical

criticism of the principle of operation of the Wire Mark Meter.

- b) The manner in which a paper surface accepts ink during the printing process is an extremely complex function of many factors, including the depth and spatial distribution of the depressions in the surface, the compressibility of the paper, and the rheological properties of the printing ink.
- c) The relationship which exists between the actual spatial distribution of printed areas on a paper surface, and the ability of the human brain to perceive a regular pattern in that distribution, is a problem of psychology which remains to be clarified.

In view of the multiplicity of factors involved in the generation and perception of wire mark on paper, there does not seem to be any reason to suppose that the power spectrum of the photodetector signal g(t) would give any better measure of the "printing wire mark" of paper than does the amplitude spectrum.

Finally, in view of the good correlations found to exist between the printing wire mark determined by visual grading, and Wire Mark Meter readings derived from the amplitude spectrum of g(t), the addition of an r.m.s. voltmeter to the analysis circuitry in order to determine the power spectrum of g(t) has not been considered worthwhile.

# 5.3 Additions to the Wire Mark Meter

One of the functions of the Wire Mark Meter included by the author in the original design specifications of the instrument was the ability to automatically plot the surface roughness spectrum of a paper sample. As the instrument developed, it became increasingly apparent that this ability would in fact be highly desirable.

The addition of a small synchronous motor and reduction gear drive to the three-gang wire-wound potentiometer of the filtering amplifier was carried out by Mr. T.S. Duchnicki. Under his supervision, a Westronics Model Sll-AT Potentiometric Strip Chart recorder was also added to record the output of the averaging amplifier. These additions proved to be extremely useful, in that they permitted the plotting of surface roughness spectra from 90 marks per inch down to 6 marks per inch in less than 90 seconds.

# 5.4 The Effect of Prism Pressure on the Surface Roughness Spectrum of Newsprint

Early surface roughness spectra plotted on a point-by-point basis had revealed that the distribution of optical contact of newsprint examined in the Chapman Printing Smoothness Tester was very sensitive to the pressure to which the sample was subjected during measurement.

In order to illustrate this effect, a series of surface roughness spectra were recorded by the author for two completely different
newsprint samples under applied pressures of 100, 300, and 500 psi. The
machine direction and cross-machine direction spectra taken on a heavily

wire-marked newsprint sample are given in Figure 18 and Figure 19 respectively; while the corresponding curves for a newsprint sample bearing an average wire mark appear in Figure 20 and Figure 21.

level of the spectra: the higher the applied pressure, the lower the average level. It is toward the high frequency end of the spectrum that this reduction is most pronounced, however, in accordance with the fact that an increase in pressure will reduce the number of small areas of contact by causing them to merge into larger ones. Note that the reduction in average level caused by a pressure increase from 100 to 300 psi is much less than the reduction in average level caused by a pressure increase from 300 to 500 psi. Further increases in the applied pressure produce progressively smaller reductions in the average level of the spectrum, in direct agreement with the variation in fractional contact area with pressure as originally described by Chapman. 5)

The spectrum of Figure 18 illustrates not only the effect of pressure on the surface roughness of newsprint, but also the phenomenon of a "frozen-in" wire mark. Note that the peak height of the curve at the fundamental machine direction wire mark frequency remains almost unaffected by a five-fold increase in the applied pressure, whereas the corresponding cross-machine direction peak height falls considerably for the same increase in pressure. For this particular newsprint the excess height index for the machine direction wire mark increases by a factor of almost two as the applied pressure increases from 100 to 500 psi.

In contrast, the peak value of the machine direction wire mark for the newsprint sample bearing only an average wire mark (Figure 20) is seen to fall with increasing pressure almost as much as the average random noise level. The excess height index for this sample is thus almost independent of the applied pressure, as are the excess heights of the cross-machine direction wire marks of both the above newsprint samples.

It is quite conceivable that the variation in the excess height wire mark index with pressure might be used as a measure of the relative "hardness" of wire mark impressions. This possibility, however, remains to be investigated.

In order to permit the intercomparison of the spectra of various newsprint papers, a prism pressure of 300 psi has been adopted as a standard value for the routine measurement of wire mark; firstly because it is typical of pressures encountered in the printing of newsprint, and secondly because little change in the surface roughness spectrum occurs with increased pressure.

#### 5.5 Reproducibility of Surface Roughness Spectra at a Single Location

Because the low frequency Y scan generator is not synchronized with the high frequency X scan generator, successive scanning rasters do not cover the same area on a sample. As a consequence, there is a certain amount of variation in the output of the averaging amplifier, whether it reads the time-average value of the output of the video amplifier or the rectified output of the filtering amplifier. As a result of this variation, successive roughness spectra taken on a given sample are slightly

different. The extent of this disagreement may be gathered from Figure 22, which shows eleven consecutive surface roughness spectra taken by the author on the same sample at three minute intervals under a constant applied pressure of 300 psi.

Each of the individual spectra has been displaced upward by an amount corresponding to 1-1/2 per cent contact area. The strong machine direction wire mark peak near 52 marks per inch shows little variation between successive runs in comparison to the weak third subharmonic component near 17 marks per inch.

The analysis of the measurements made on the eleven curves gave the following results:

	Mean Value	Standard Deviation
Peak Height of Fundamental Wire Mark Peak	9.6%	.25%
Random Noise Level Adjacent to Fundamental Wire Mark Peak	5.1%	.14%
Excess Height of Fundamental Wire Mark Peak	4.5%	.25%

In view of the known variability in the properties of paper with location, these results are considered to be quite acceptable. If desired, the precision of the measurement may be enhanced by using a longer time constant in the averaging amplifier, coupled with a slower rate of rotation of the filtering amplifier frequency control.

In order to determine the optimum time to scan through the frequency spectrum of a given type of paper, however, it would be necessary

to have some idea of the variability of the surface roughness spectrum from one location to another for that type of paper. Preliminary studies on newsprint seem to suggest that with the present combination of averaging amplifier time constant and rate of frequency scanning, time is better spent in taking separate spectra at several different locations rather than attempting to determine the spectrum precisely at one particular location.

#### VI : DISCUSSION, POSSIBLE IMPROVEMENTS, AND CONCLUSION

# 6.1 General Discussion

The Wire Mark Meter has now been in use as a laboratory instrument at the Institute for almost one and one-half years. During that time it has yielded considerable insight into the surface roughness of newsprint under pressure and the problem of wire mark in Canadian newsprint papers. A technical report describing the instrument and some of its findings has been published. 12)

An intensive study of the problem of wire mark in newsprint, involving a comprehensive survey of commercial Canadian newsprint papers with the Wire Mark Meter, is currently being undertaken by Mr. T.S. Duchnicki. 10)

Preliminary results of additional work by the same author would seem to suggest that a very high correlation may exist between the random noise level of a surface roughness spectrogram of a newsprint sample at frequencies well-removed from the fundamental wire mark peaks, and the overall printability of the sample as judged by visual grading. If this should indeed turn out to be the case, the possibility exists that the Wire Mark Meter might find application as a "nonprinting" predictor of the printability of newsprint.

The general opinion of the instrument would thus seem to be that it is a highly successful research tool for the study of wire mark, and that it holds considerable promise as an instrument for studying the

relationships between the surface contact of paper under pressure and its final printability.

In spite of its success in the laboratory, however, the operating principle of the Wire Mark Meter does not appear to lend itself to immediate application in the paper mill. Even if continued use of the instrument in the laboratory succeeds in delineating the rôles of the various factors involved in the generation of wire mark on paper, the nature of the optical system and the time requirements of the analysis process would appear to preclude the use of the Wire Mark Meter for the monitoring, recording, or controlling of the wire mark on paper while it is moving.

#### 6.2 Possible Improvements to the Wire Mark Meter

Experience with the Wire Mark Meter has shown that the utility of the instrument could be greatly enhanced by certain modifications and improvements to the optical, hydraulic, and electronic systems of the instrument. With regard to the electronics systems, considerable improvement could be made in both the scan generation and analysis circuitry.

# 6.2.1 Possible Improvements in the Optical System of the Wire Mark Meter

The most serious of all the changes in the instrument which have been proposed so far would be the complete redesign of the optical system of the Chapman Printing Smoothness Tester to adapt it specifically for use in the Wire Mark Meter. Because there is no need for the upper photocell used in the Chapman instrument, (Figure 2), the corresponding upper face

of the compound prism could be completely eliminated. With a suitable relocation of the photomultiplier tube, and a reduction in the length of the lower face of the compound prism, the main prism block could be reduced in height from four inches to less than three. As a consequence, the focal length of the main focussing lens could be reduced, and the lens and flying-spot C.R. tube brought much closer to the prism. The resultant optical system would be far less cumbersome than the present one.

Better orientation of the photomultiplier tube with respect to the compound prism and the introduction of a suitably located aperture could both be used to maintain the average level of the reflected light signal seen by the photomultiplier tube essentially constant over the entire area being scanned. Credit for the latter suggestion is due to Mr. J.G. Buchanan.

In addition, the area scanned could be made at least one inch square at the paper surface, so that both machine direction and cross-machine direction spectra could be recorded on the same sample simply by rotating the scanning raster. This feature would be particularly useful in the analysis of small experimental paper samples made in the laboratory.

# 6.2.2 Possible Improvements in the Hydraulic System

Considerable improvement could also be effected in the hydraulic system used to apply pressure to the lower glass backing plate. Changing the present system to an air-loaded type would permit constant pressure loading of the paper sample, and would eliminate the gradual relaxing of

the applied pressure which occurs in the present design as the paper yields in compression during the first few minutes after loading. If this air-loading of the hydraulic system were performed by selecting the output of one of several fixed low-pressure air regulators, (set for example to give prism pressures of 100, 300, or 500 psi), good reproducibility of the applied pressure could be obtained on all samples, and the annoying problem of accidentally overshooting the desired pressure largely overcome.

# 6.2.3 Possible Improvements to the Scan Generation Circuitry

Insofar as the scan generation circuitry is concerned, the problem of deflecting the beam in the flying-spot C.R. tube is essentially a problem of obtaining a sufficient number of ampere-turns in the deflection yoke. Although direct coupling to the yoke must be used, it is extremely wasteful to employ two D.C. power amplifiers dissipating over one hundred watts in their output stages alone to drive a load consuming less than five watts of actual power. Because thermal drift is such a problem in both the present scan generation and analysis circuitry, the elimination of the existing sweep circuit power amplifiers would be highly desirable.

One possible alternative would be to replace the present highimpedance deflection yoke with a low-impedance type, and to drive it by
means of direct-coupled push-pull power transistors. Linearity of the
deflection currents could be achieved in the same manner as with the
present system; that is to say, by using negative current feedback through
high-gain operational amplifiers. Solid-state plug-in operational

amplifiers are now commercially available and would be a natural choice for this function.

Because of the higher deflection yoke currents involved in a low-impedance system however, and the susceptibility of transistors to failure from high transient reverse voltages, careful attention would have to be paid to the damping of the deflection yoke in such a system.

One very attractive possibility that should be investigated is the use of the operational amplifier - power output stage combination as an integrator with which to derive the triangular-wave deflection voltages directly, instead of deriving them from an R-C network. In order to do this, the current feedback path could be made through a large capacitor, while the input impedance to the operational amplifier would be purely resistive. The input signal fed to this combination would then have to be a true zero mean-value square wave, or else the average level of the output current would drift continuously. This latter problem could be avoided by parallelling the output capacitor with a suitable resistance, so that the D.C. gain of the system remains fixed. In this way the average level of the output current could be set by varying the average value of the input square wave signal, while the gain of the overall system could be adjusted by varying the current feedback resistor, as is done in the present system.

Two transistorized bistable D.C.-coupled multivibrators for the generation of the required X and Y sweep circuit square wave signals would normally present little problem, but the "on" and "off" collector voltage levels of such multivibrators would undoubtedly be highly

temperature sensitive. This latter difficulty would be even more acute than it is with the present vacuum tube circuitry. One possible way of avoiding the problem however, might be to use a pair of low temperature-coefficient zener diodes connected back-to-back in order to define the peak values of the square wave signals fed to the following circuitry.

Triggering of the X sweep multivibrator at 120 cps would be most conveniently done by differentiating a clipped and full-wave rectified sine wave signal derived from the power line voltage.

Only one function would then remain to be provided: that of a low-frequency square wave oscillator for the Y scan generator. Ideally, this function would be provided by additional solid-state circuitry in order to simplify the overall power supply requirements of the instrument.

One possible solution to this problem could be provided by a system devised by the author for the low-frequency pulsing of a small rotary solenoid. The device provides a choice of pulses at several different repetition rates between 1/4 and 2 cps, all in time synchronism with the power line frequency. Basically all that is required is a small synchronous clock motor driving a six to eight inch diameter opaque disk inside a light-tight enclosure. Small pilot lights set at various radii from the center of the disk are mounted facing one side of the disk, while light-dependent resistors are mounted opposite the pilot lights on the other side. Small holes are drilled in the disk at the appropriate radii. The rate of rotation of the disk and the number of holes at a given radius are the determining factors in setting the repetition rate of the light flashes on the various light-dependent resistors.

In this application, a choice of three or four photo-resistors could be provided; with the desired one selected by connecting it into a suitable R-C network to provide triggering pulses to the Y sweep multi-vibrator. The basic system is capable of supplying pulses at fixed repetition rates over a frequency range of at least ten-to-one, and has the two virtues of being both temperature independent and synchronized with the power line frequency. In the present case, this latter feature would ensure that the same path would always be swept out on a given paper sample, and would thus help to further reduce the variation in the average level of the photomultiplier tube signal.

# 6.2.4 Possible Improvements in the Analysis Circuitry

Considerable improvement could also be made to the analysis circuitry of the Wire Mark Meter along the same lines as suggested above for the scan generation circuitry.

One of the most obvious steps that could be taken would be to replace the vacuum tube operational amplifier used as a video amplifier with a solid-state plug-in unit. Several of the models now commercially available are true current amplifiers, and would thus be ideally suited to the problem of amplifying the weak photomultiplier tube current-source signal. Because such a module would generate neither heat nor light, and should require infrequent checking, it could be profitably mounted in the same enclosure as the photomultiplier tube itself. The overall bandwidth of the video amplifier would then no longer depend on the effective capacitance of the shielded cable running from the P.M. tube and prism

housing to the rest of the analysis circuitry.

The second obvious step to be taken in improving the analysis circuitry would be the replacement of the present vacuum tube averaging amplifier with its solid-state counterpart. Little problem ought to be encountered in this step.

Far more thought would have to go into modification of the filtering amplifier section of the analysis circuitry. Now that the operating principle of the Wire Mark Meter has proven itself in the laboratory, and now that the characteristics of the filtering amplifier are fairly well defined, the best procedure would seem to be to incorporate into the instrument a commercial audio frequency spectrum analyzer. In order to do this, however, an instrument must be found that has constant gain and constant Q from at least 500 cps up to 10 KC. or more; and which could also be modified to allow for semicontinuous mechanical tuning. Ideally, such an instrument would include provision for a continuously variable Q up to a value of at least 20. With such a feature, the effect of altering the electrical resolution of the analysis circuitry could be readily investigated. Finally, since most commercial audio spectrum analyzers include a quasi-r.m.s. detector and output indicator, it would be necessary to gain access directly to the output of the filter circuitry. (If such a detector were included, however, it would be very interesting to actually compare the wire mark indices derived from the relative amplitude spectra and relative power spectra of a series of unprinted paper samples, with the visual grading of a similar set of printed samples.) To avoid the need for recalibration of the filtering amplifier every time a change in its gain is required, provision should also be made to include a calibrated attenuator network at the output of the video amplifier section of the analysis circuitry. If this step were taken, the external calibrating circuitry would then be needed only for occasional checking of the analysis circuitry.

One final area of the analysis circuitry would then remain to be improved: that of the auxiliary strip-chart recorder. It would be most convenient to have the semi-automatic tuning of the spectrum analyzer start and stop the recorder chart-drive motor, and to have special chart paper printed with the time axis corresponding to the calibration of the filter of the spectrum analyzer.

## 6.3 Conclusion

The development of the Wire Mark Meter has been a most stimulating and rewarding project. From the time of its inception almost three years ago, the project has involved problems in optics, mechanics, electronics and paper technology.

It is the author's fond hope that the development of the Wire Mark Meter will prove to be a significant contribution to the field of pulp and paper research.

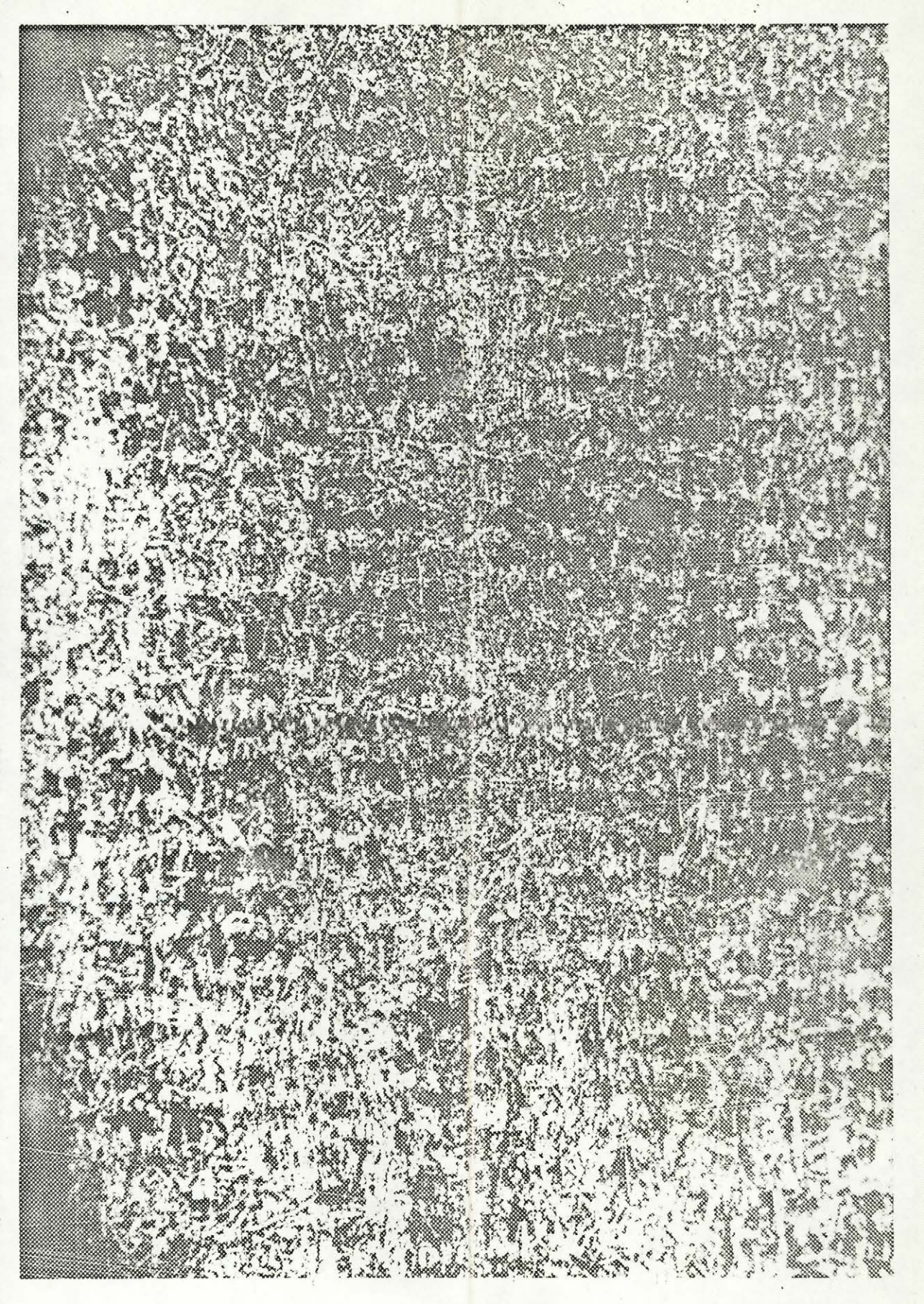
## BIBLIOGRAPHY

- 1. Parker, J.R. and Attwood, D. Paper Tech. 2, No. 5: T191-T198 (481-488) (1961).
- 2. Burkhard, G., Wrist, P.E. and Mounce, G.R. Tech. Sect., CPPA Proc. 221-238 (1960).
- Sankey, C.A. and Foss, L.E. Pulp Paper Mag. Can. <u>62</u>, No. 12:
   T519-T531 (1961).
- 4. Chapman, S.M. Pulp Paper Mag. Can. 55, No. 4: 88-93 (1954).
- 5. Chapman, S.M. Pulp Paper Mag. Can. 48, No. 3: 140-150 (1947).
- 6. Tucker, M.J. Brit. Jr. App. Phys. 8, 137-142 (April, 1957).
- 7. Koerner, H. Electronics. Nov. 11: 91-92 (1960).
- 8. Cowles, L.G. Proc. I.R.E. 40, 1712-1717 (1952).
- 9. Smith, K.C.A. Ph.D. Diss. Cambridge (1957).
- 10. Duchnicki, T.S. PPRIC Proj. 61-4 (Unpublished Work).
- 11. Steinberg, S., Geffken, C.F. and Herman, W.K. Tappi. <u>43</u>, No. 6: 539-552 (1960).
- 12. Lindsay, R.A., Duchnicki, T.S. and Buchanan, J.G. PPRIC Tech. Rep. No. 319.

## LIST OF FIGURES

Figure	1.	Newsprint Sample Viewed Through Inspection Port of Chapman Printing Smoothness Tester	70
Figure	2.	Optical System of the Chapman Printing Smoothness Tester	71
Figure	3.	Photodetector Signal Waveforms	72
Figure	4.	X and Y Sweep Waveforms	73
Figure	5.	Proposed Optical System of the Wire Mark Meter	74
Figure	6.	Proposed Block Diagram of Wire Mark Meter	75
Figure	7.	Basic Sweep Circuitry	76
Figure	8.	Sweep Oscillator Waveforms	77
Figure	9.	Overall View of Wire Mark Meter	78
Figure	10.	Basic Filter Circuitry	79
Figure	11.	Surface Roughness Spectrum of Newsprint Having Strong Wire Mark (Machine Direction)	80
Figure	12.	Surface Roughness Spectrum of Newsprint Having Strong Wire Mark (Cross-Machine Direction)	81
Figure	13.	Surface Roughness Spectrum of Newsprint Having Average Wire Mark (Machine Direction)	82
Figure	14.	Surface Roughness Spectrum of Newsprint Having Average Wire Mark (Cross-Machine Direction)	83
Figure	15.	Surface Roughness Spectrum of Newsprint Having Weak Wire Mark (Machine Direction)	84
Figure	16.	Surface Roughness Spectrum of Newsprint Having Weak Wire Mark (Cross-Machine Direction)	85
Figure	17.	Possible Wire Mark Indices	86

Figure	18.	Effect of Prism Pressure on Newsprint Having Strong Wire Mark (Machine Direction)	87
Figure	19.	Effect of Prism Pressure on Newsprint Having Strong Wire Mark (Cross-Machine Direction)	88
Figure	20.	Effect of Prism Pressure on Newsprint Having Average Wire Mark (Machine Direction)	89
Figure	21.	Effect of Prism Pressure on Newsprint Having Average Wire Mark (Cross-Machine Direction)	90
Figure	22.	Reproducibility of Surface Roughness Spectra Taken at a Single Location	91



NEWSPRINT SAMPLE VIEWED THROUGH INSPECTION PORT OF CHAPMAN PRINTING SMOOTHNESS TESTER FIGURE 1.

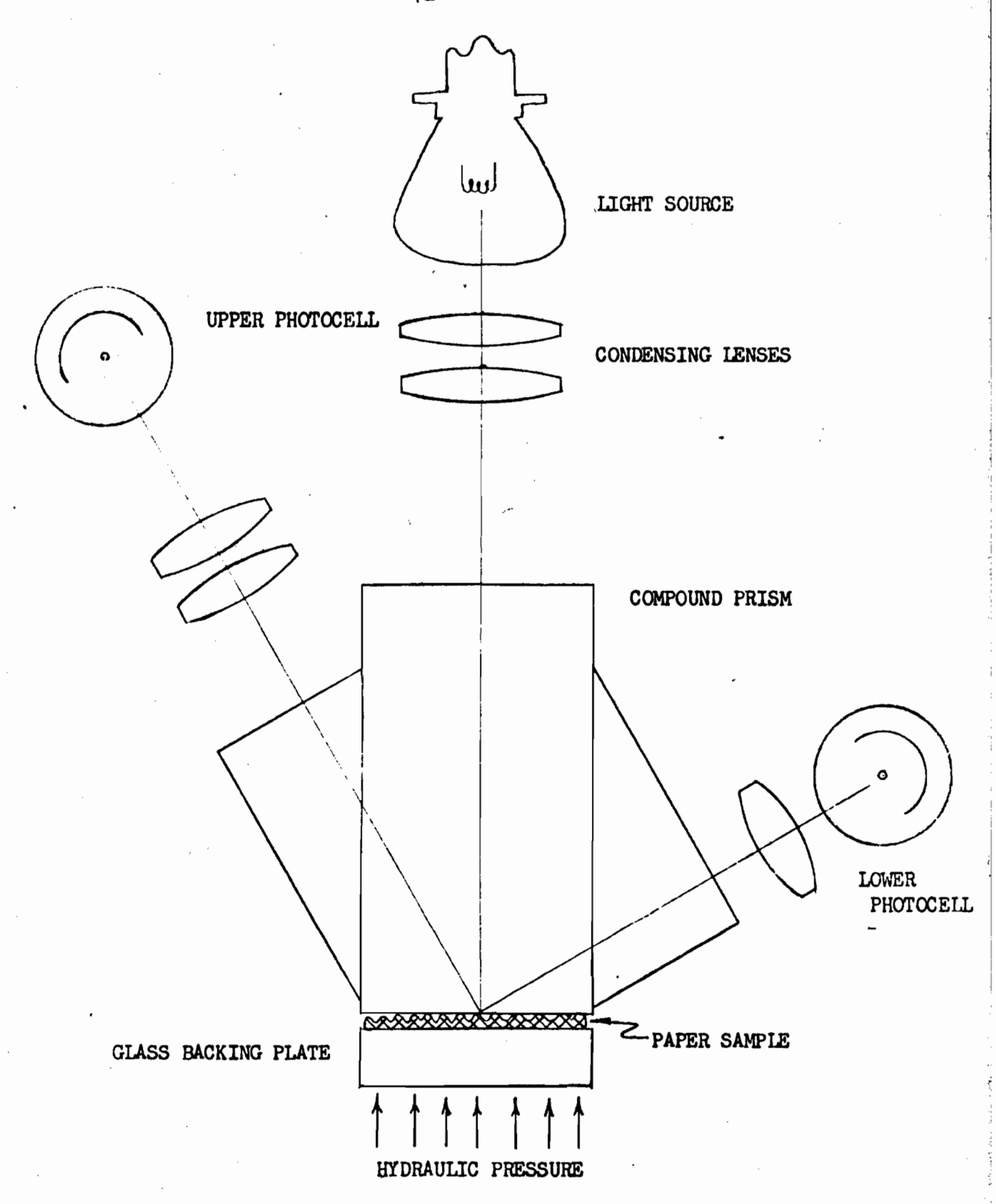
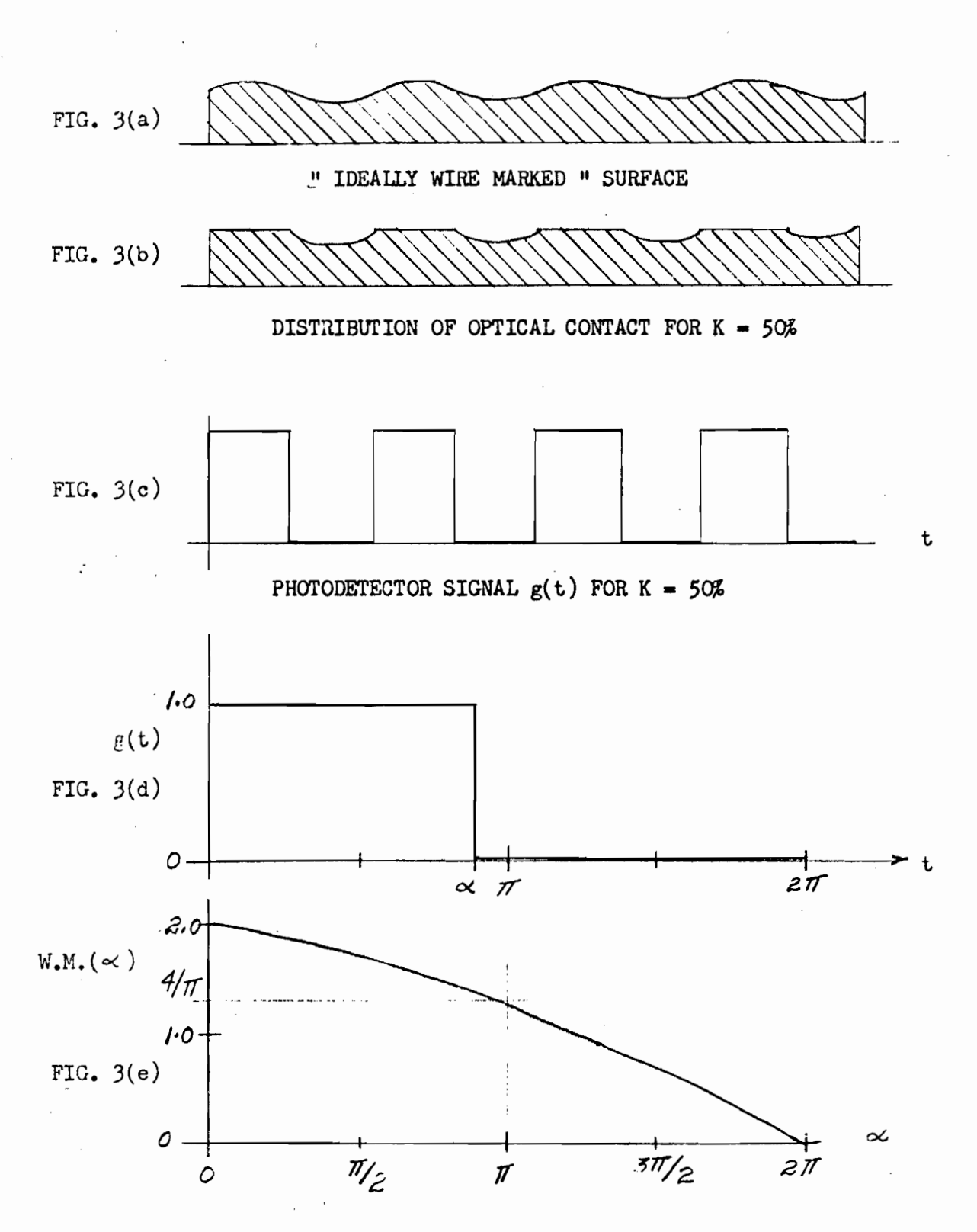
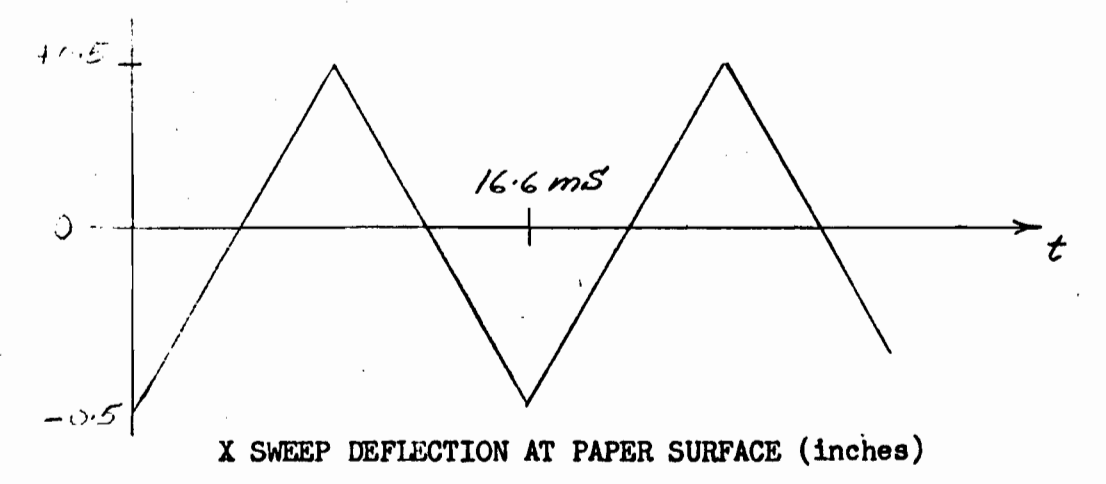
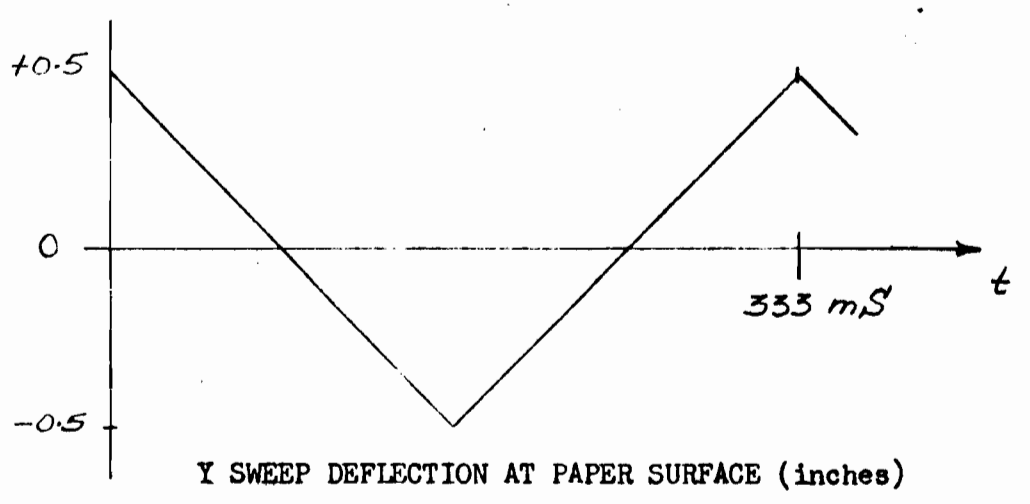


FIGURE 2. OPTICAL SYSTEM OF THE CHAPMAN PRINTING SMOOTHNESS TESTER









RESULTANT SCAN

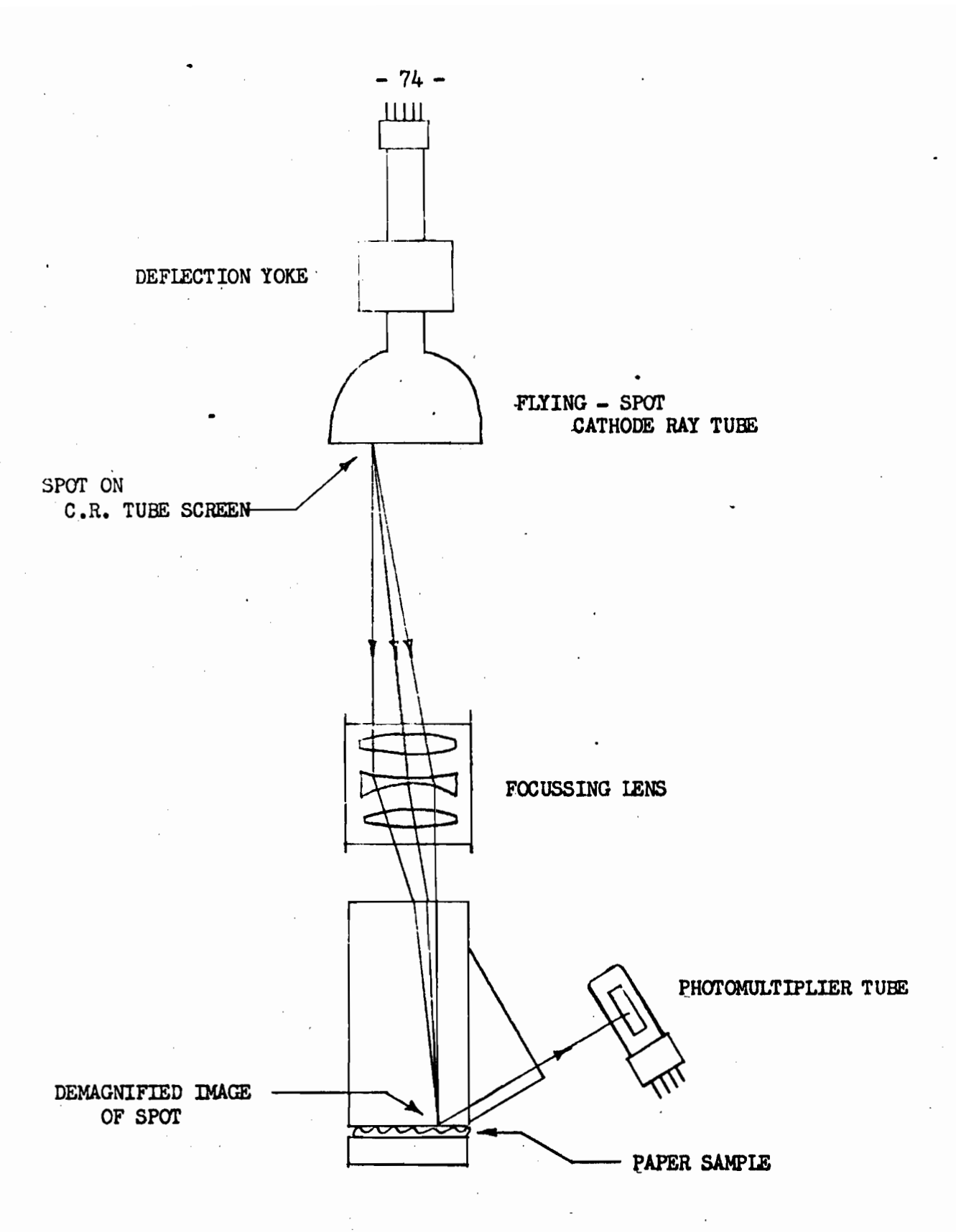


FIGURE 5. PROPOSED OPTICAL SYSTEM OF THE WIRE MARK METER

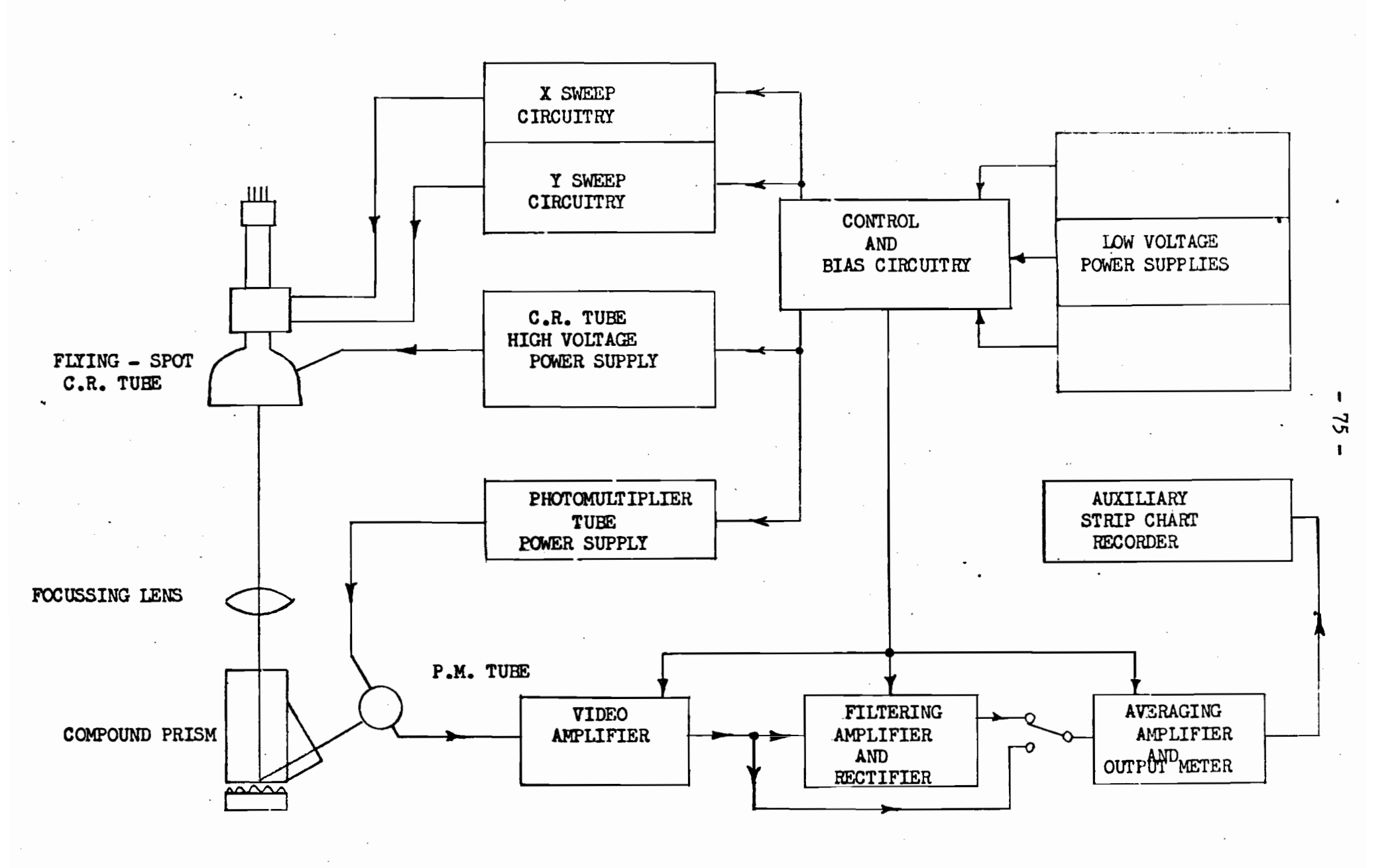
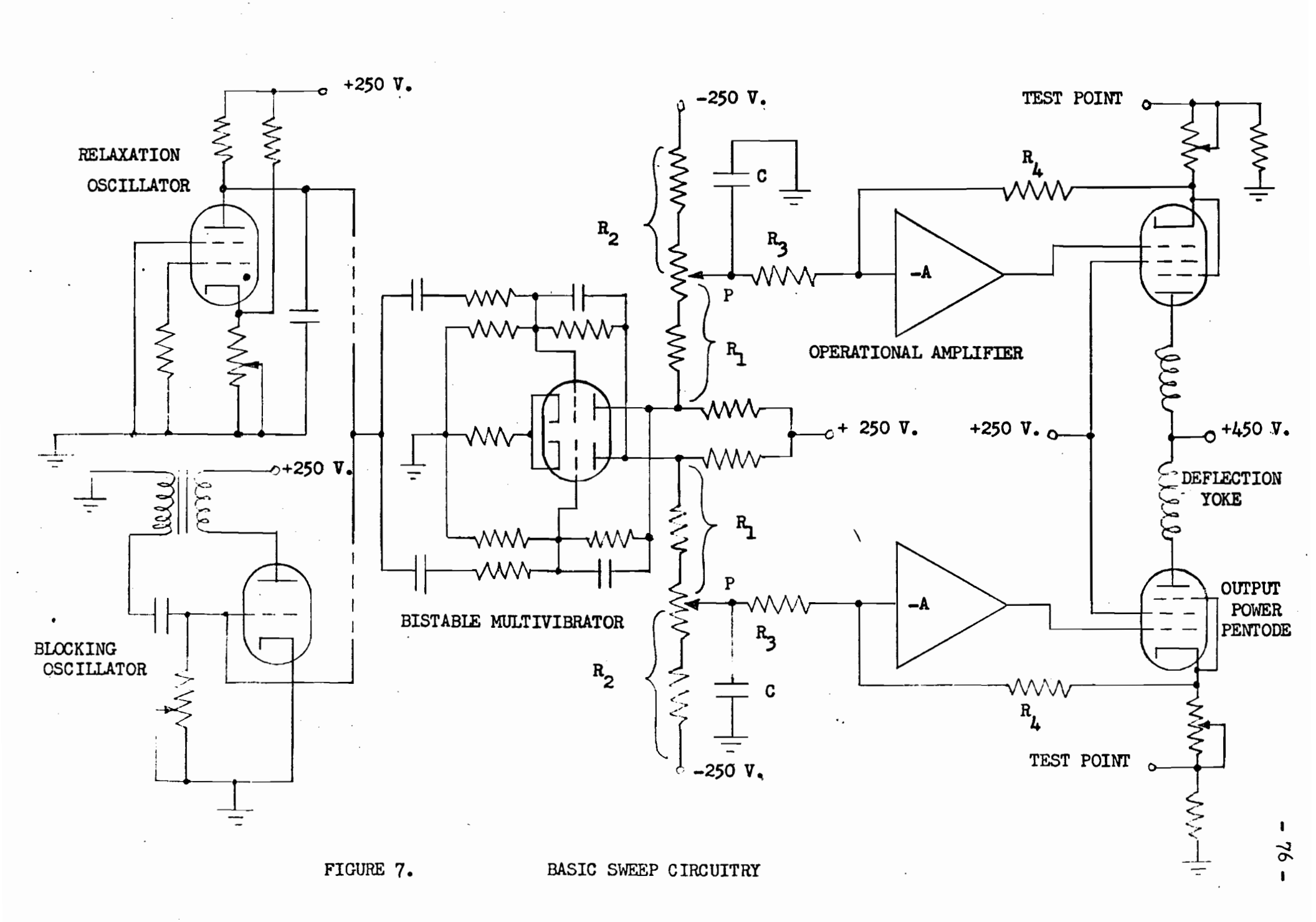


FIGURE 6.



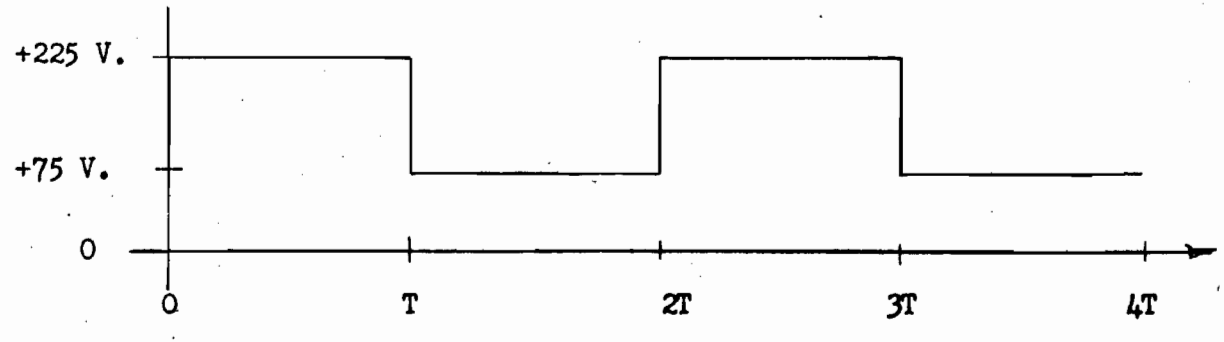
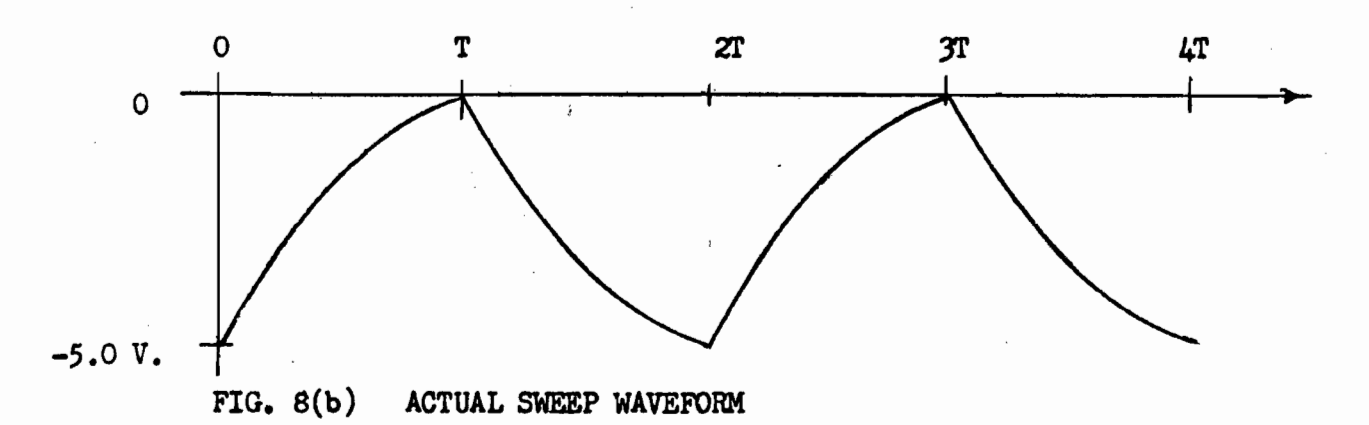
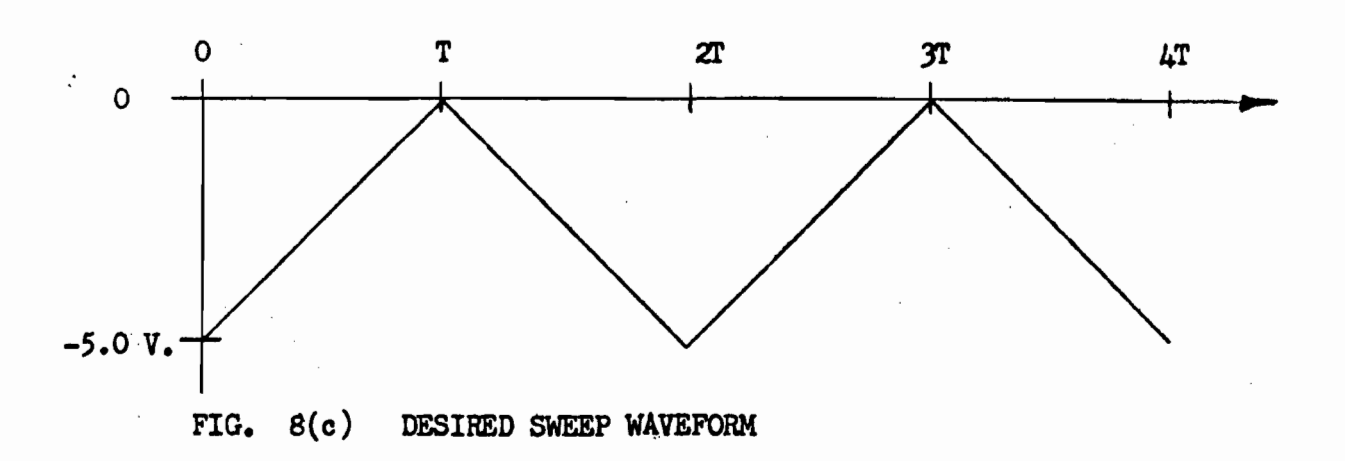


FIG. 8(a) MULTIVIBRATOR PLATE VOLTAGE WAVEFORMS





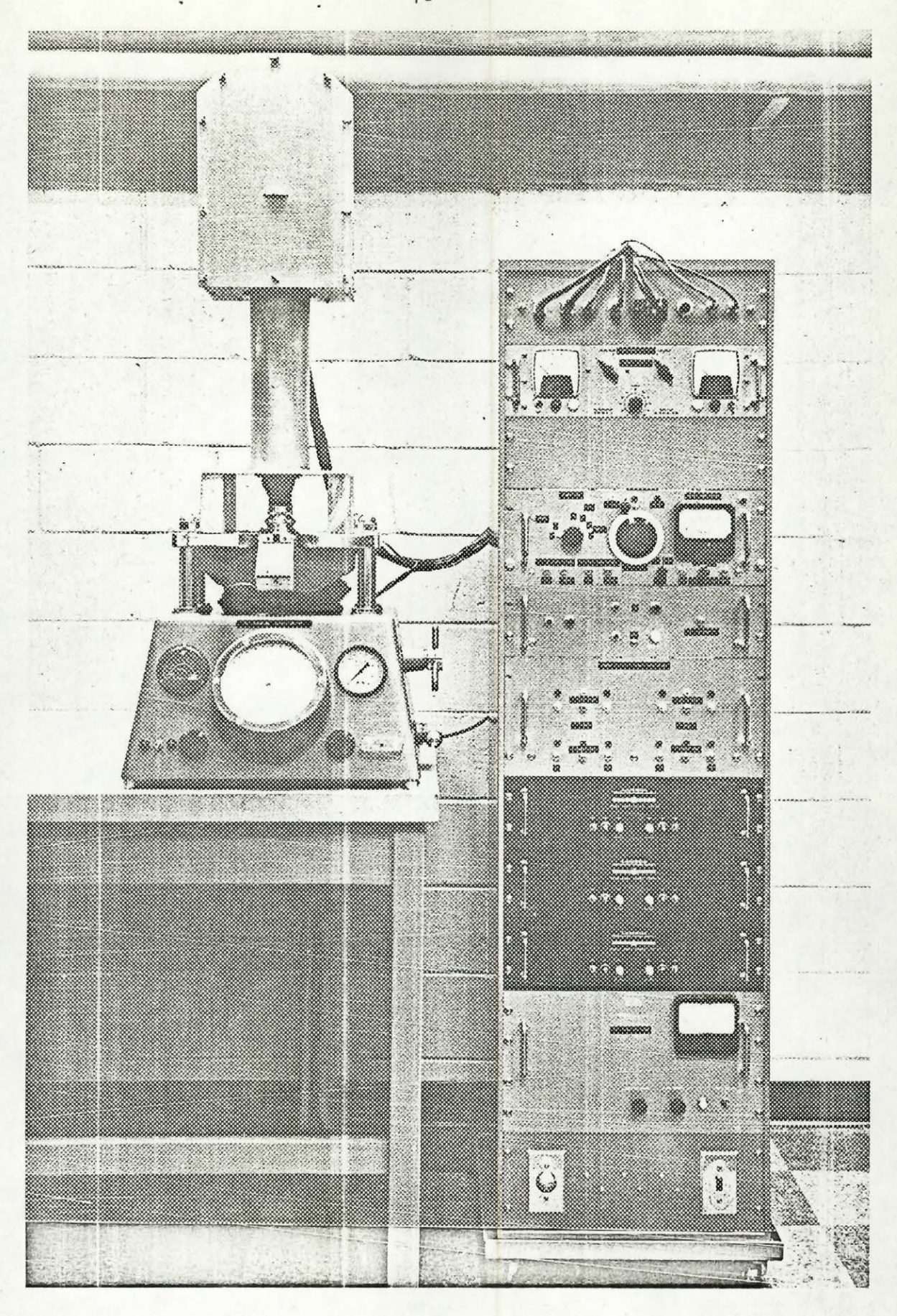
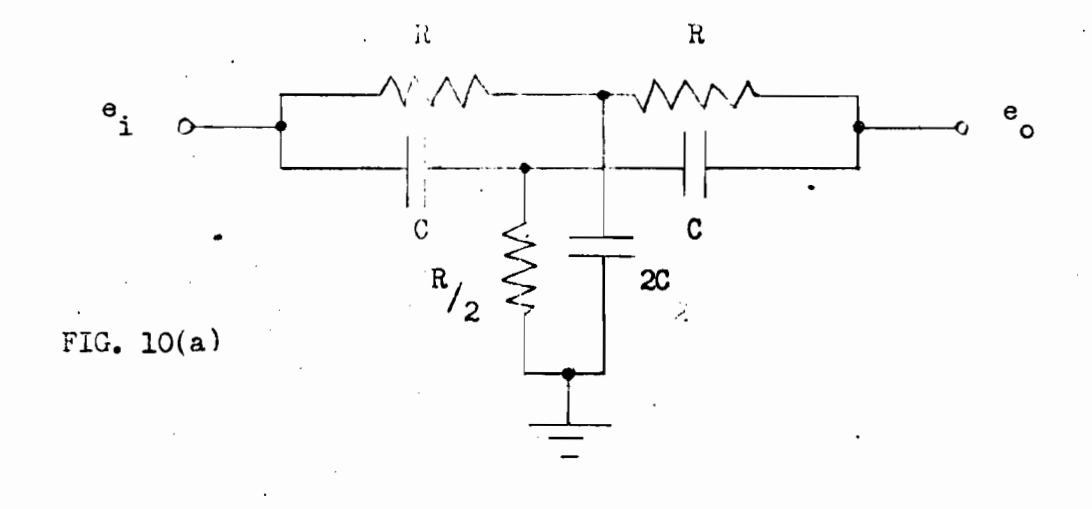
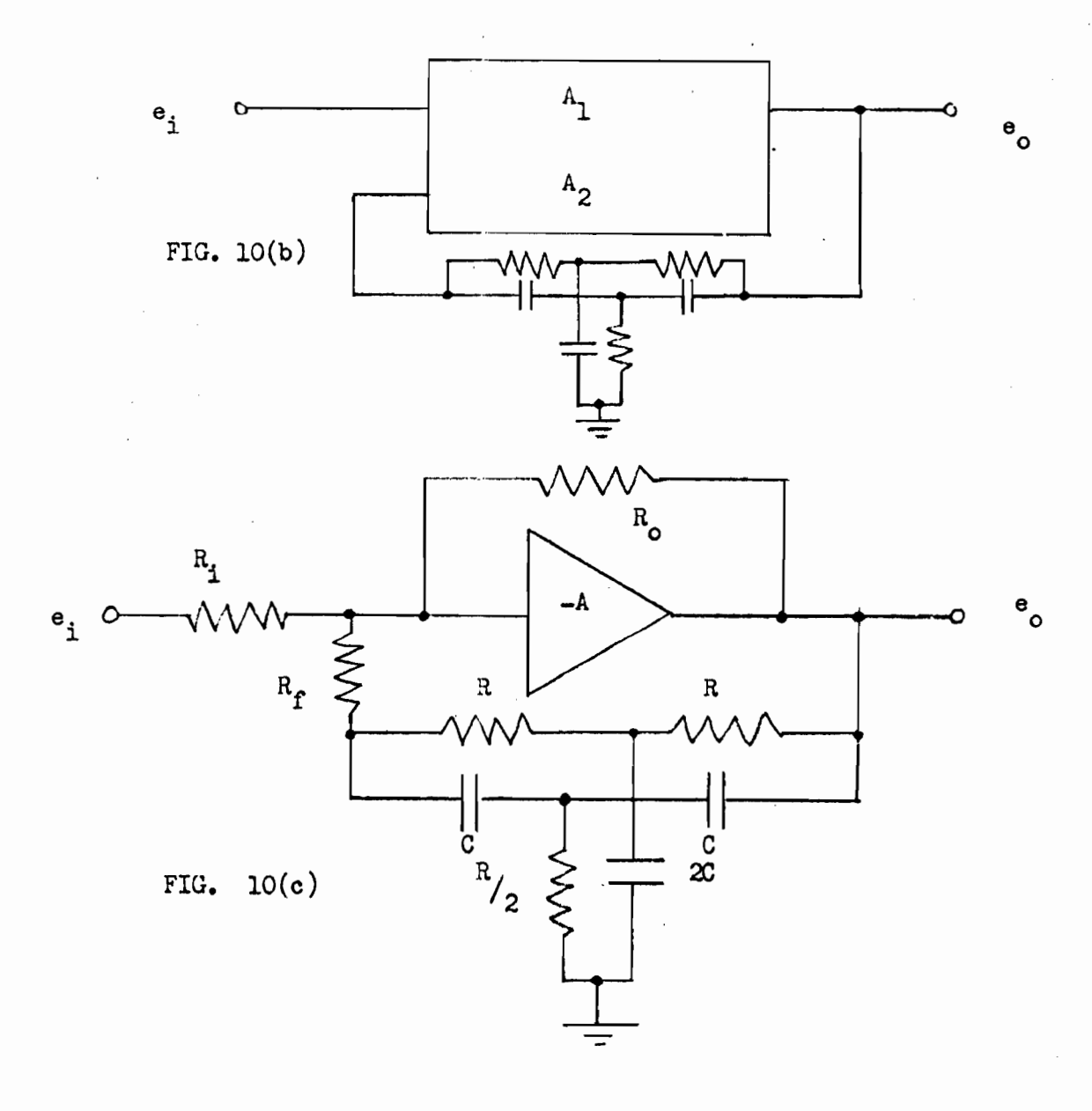


FIGURE 9. OVERALL VIEW OF WIRE MARK METER





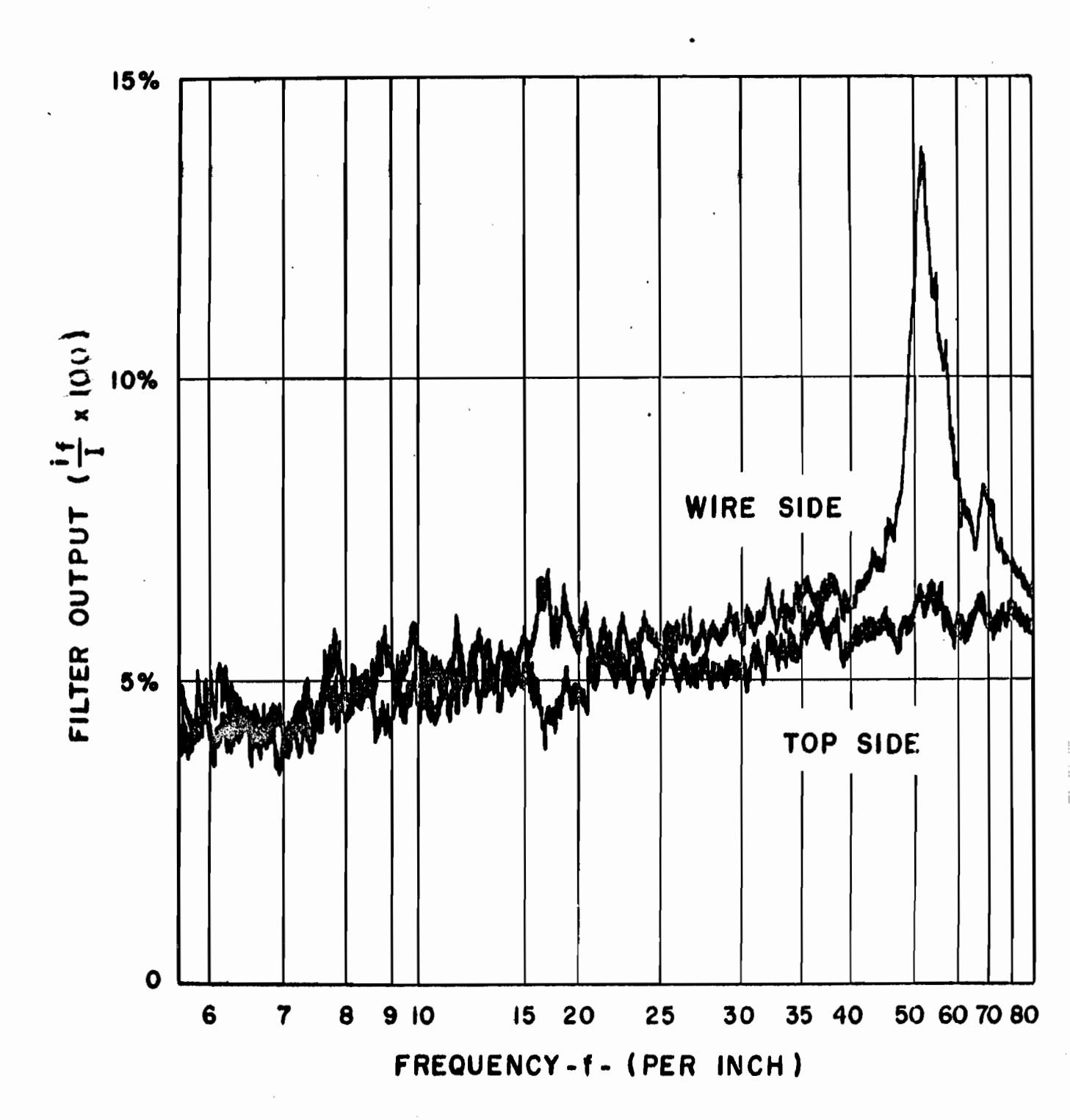


FIGURE 11 SURFACE ROUGHNESS SPECTRUM OF NEWSPRINT HAVING STRONG WIRE MARK (MACHINE DIRECTION)

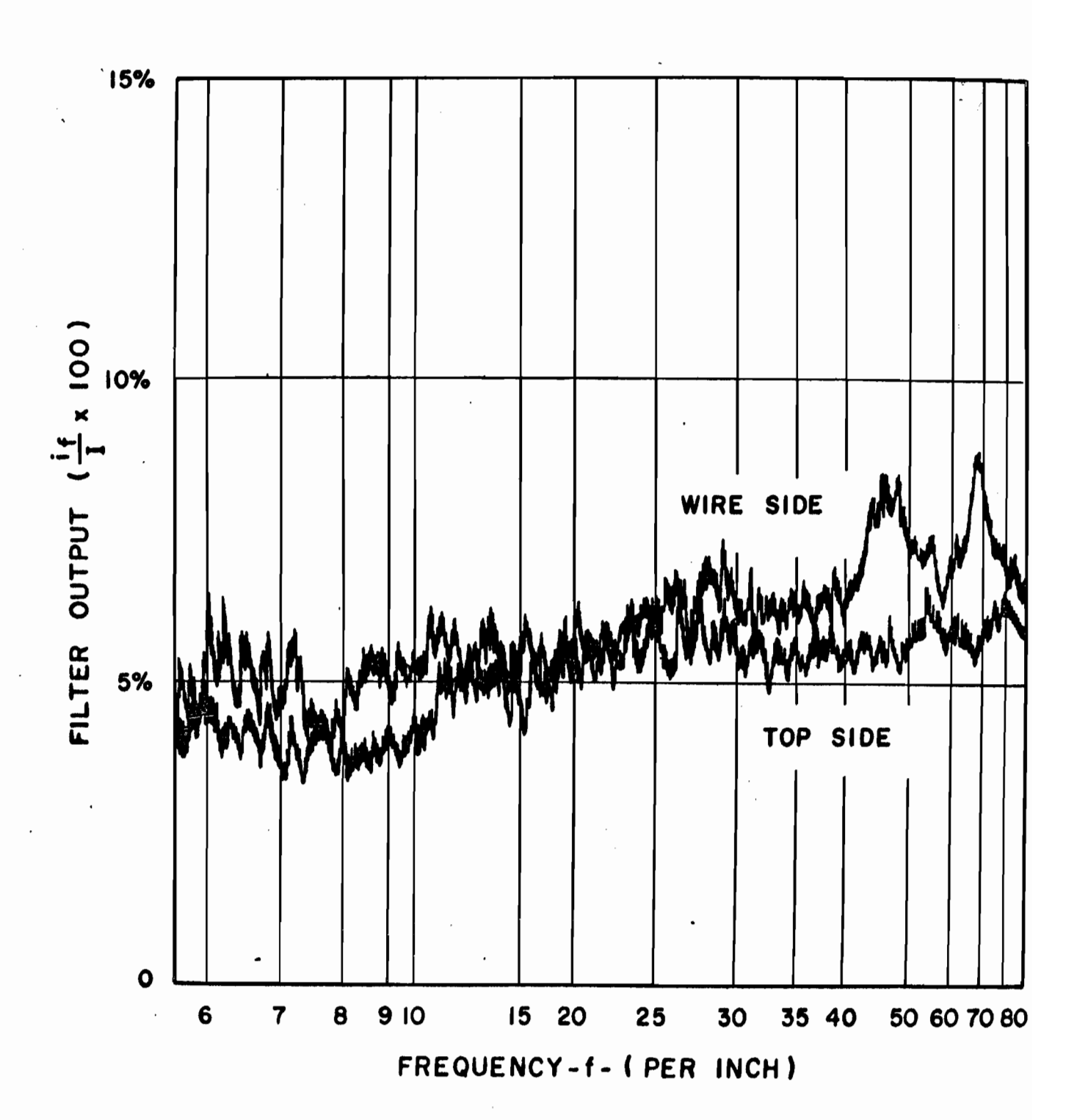


FIGURE 12 SURFACE ROUGHNESS SPECTRUM OF NEWSPRINT HAVING STRONG WIRE MARK (CROSS-MACHINE DIRECTION)

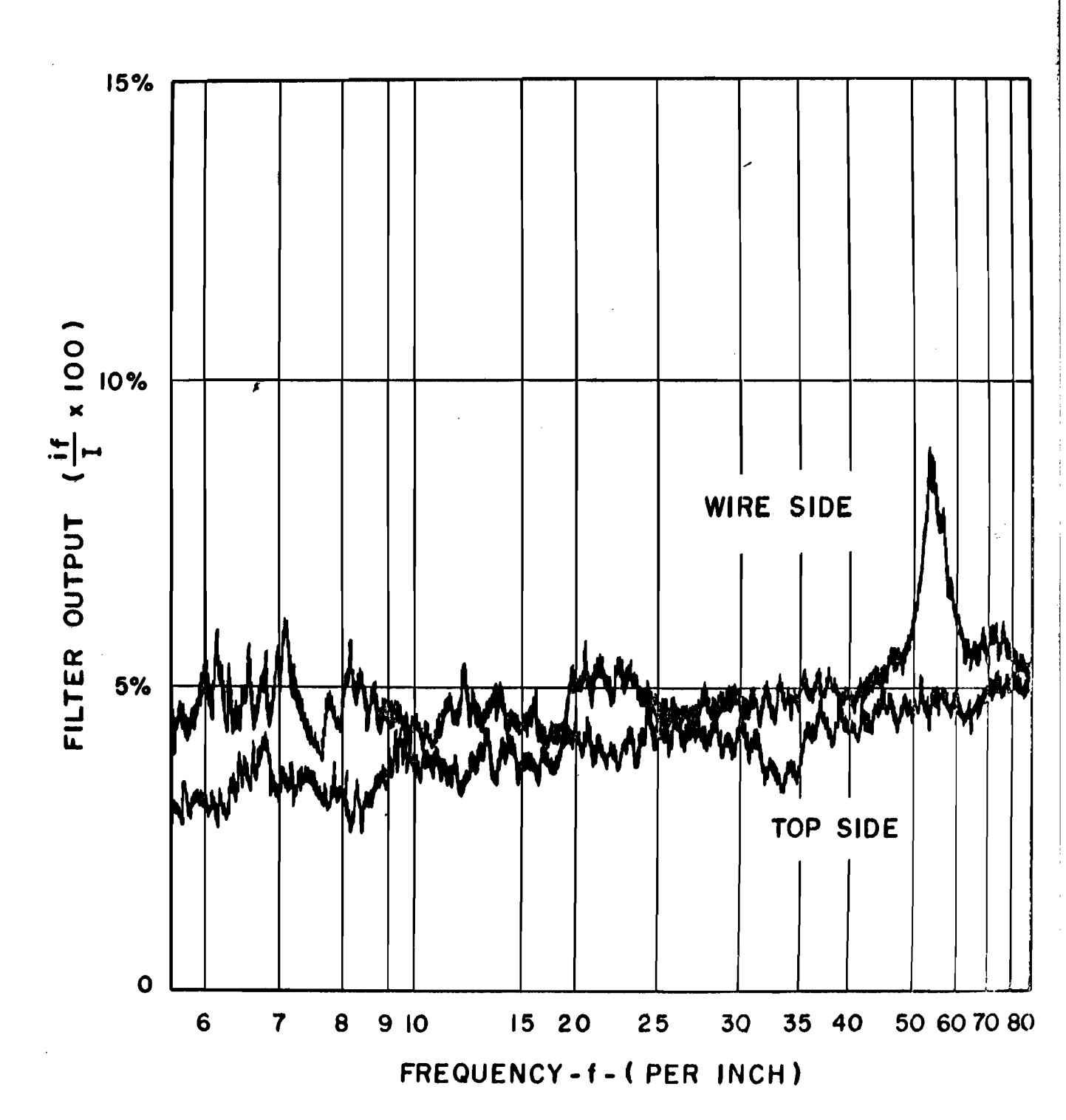
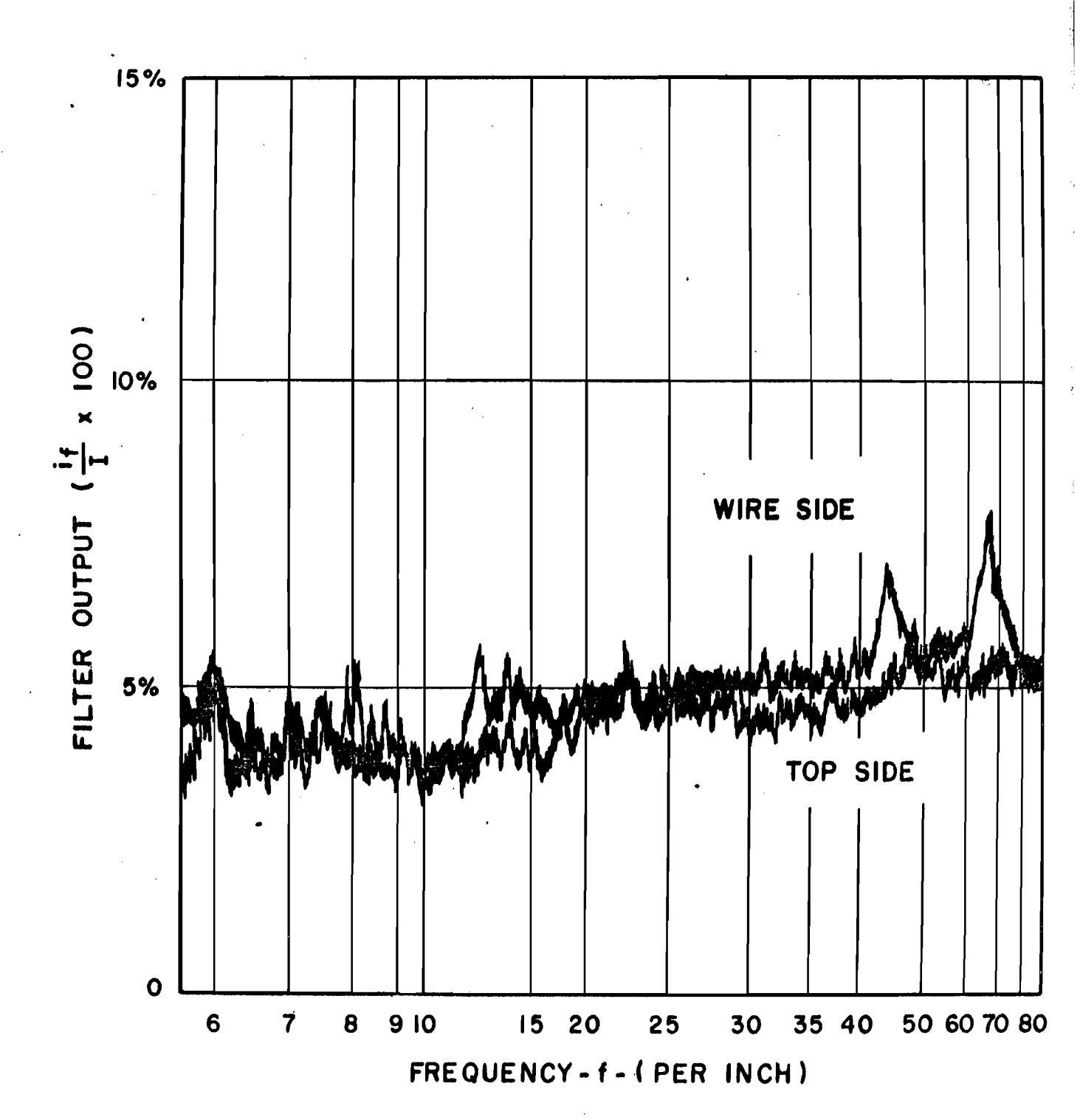


FIGURE 13 SURFACE ROUGHNESS SPECTRUM OF NEWSPRINT HAVING AVERAGE WIRE MARK (MACHINE DIRECTION)



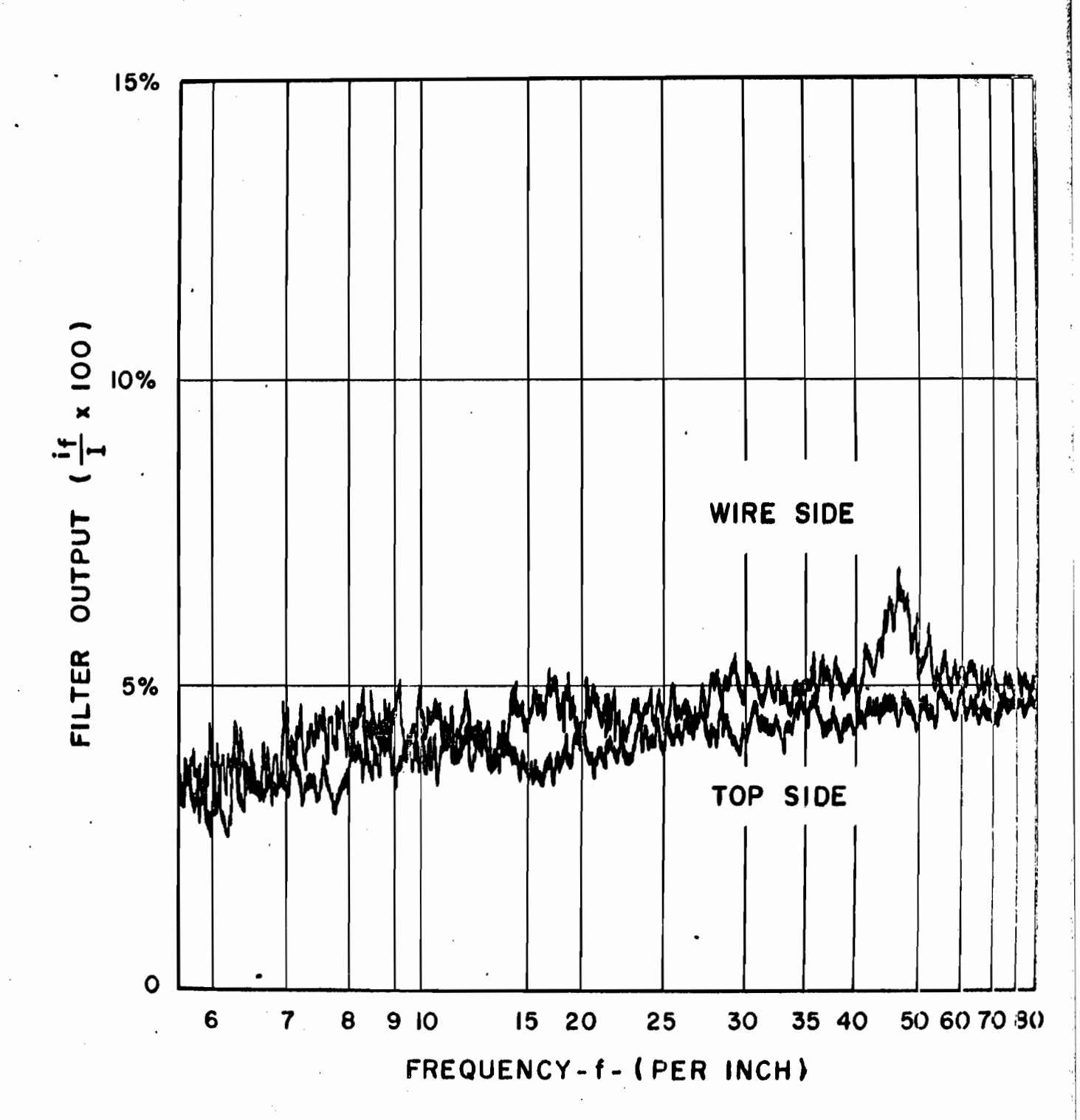


FIGURE 15 SURFACE ROUGHNESS SPECTRUM OF NEWSPRINT HAVING WEAK WIRE MARK (MACHINE DIRECTION)

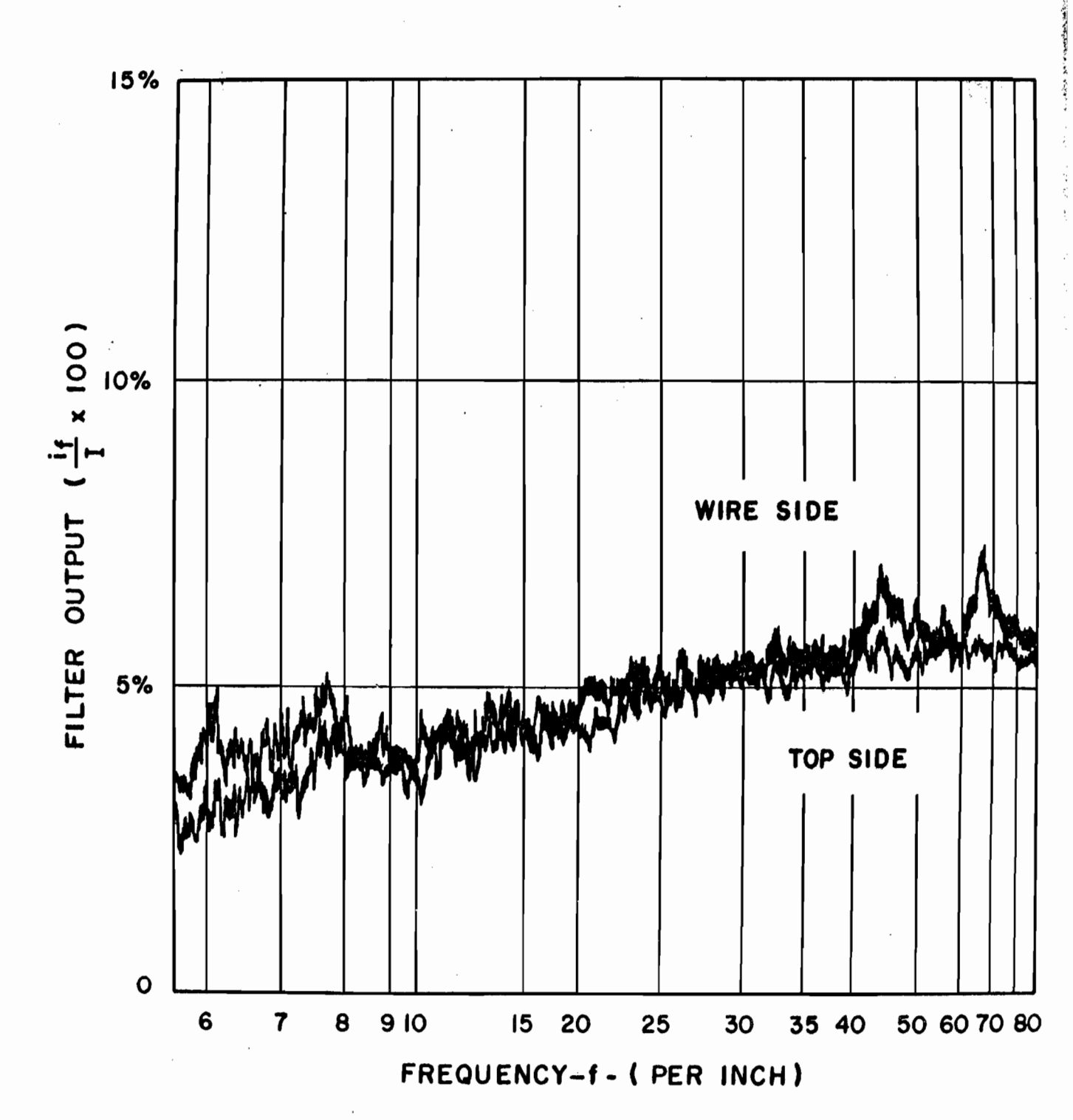
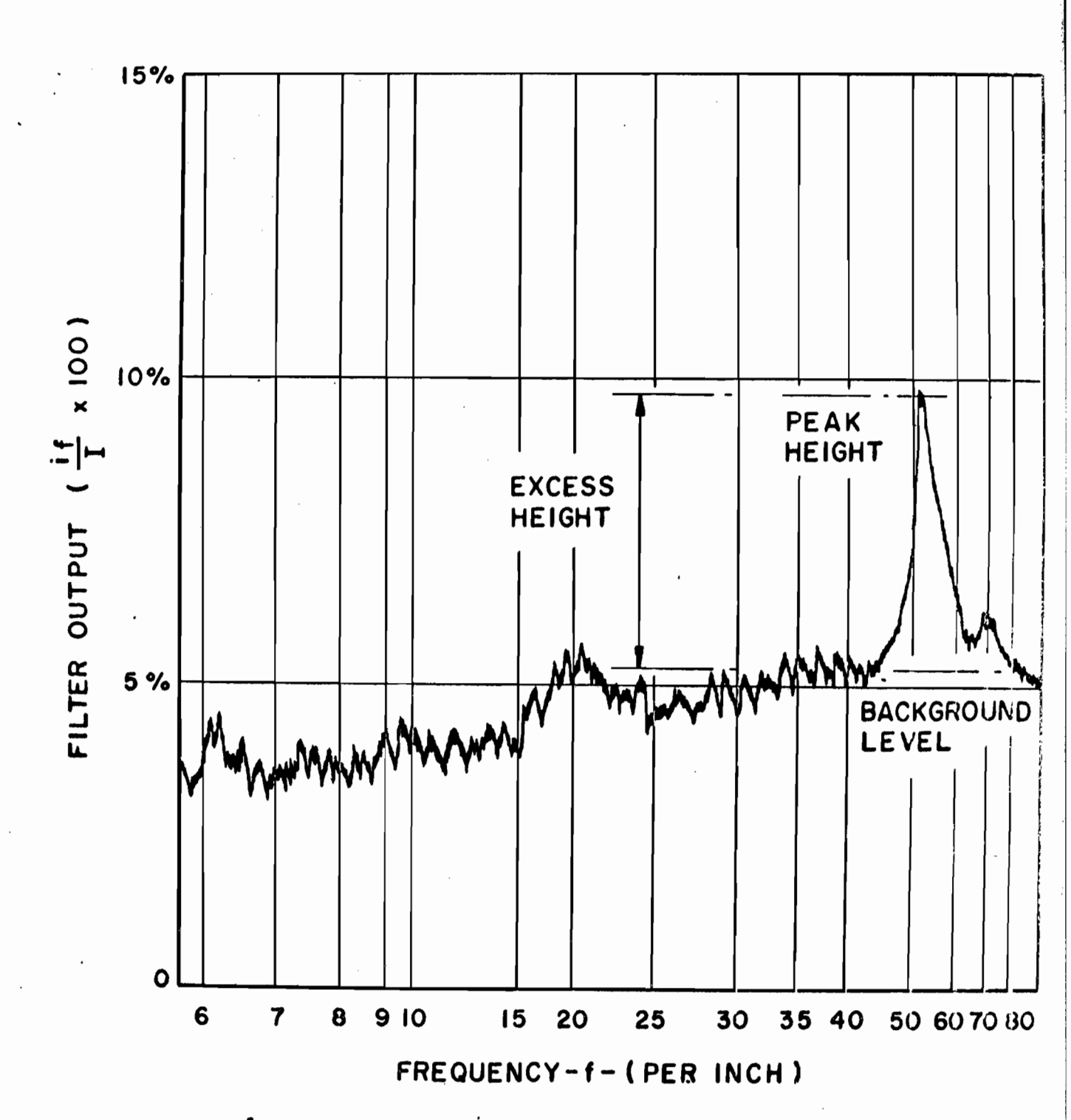


FIGURE 16 SURFACE ROUGHNESS SPECTRUM OF NEWSPRINT HAVING WEAK WIRE MARK (CROSS-MACHINE DIRECTION)



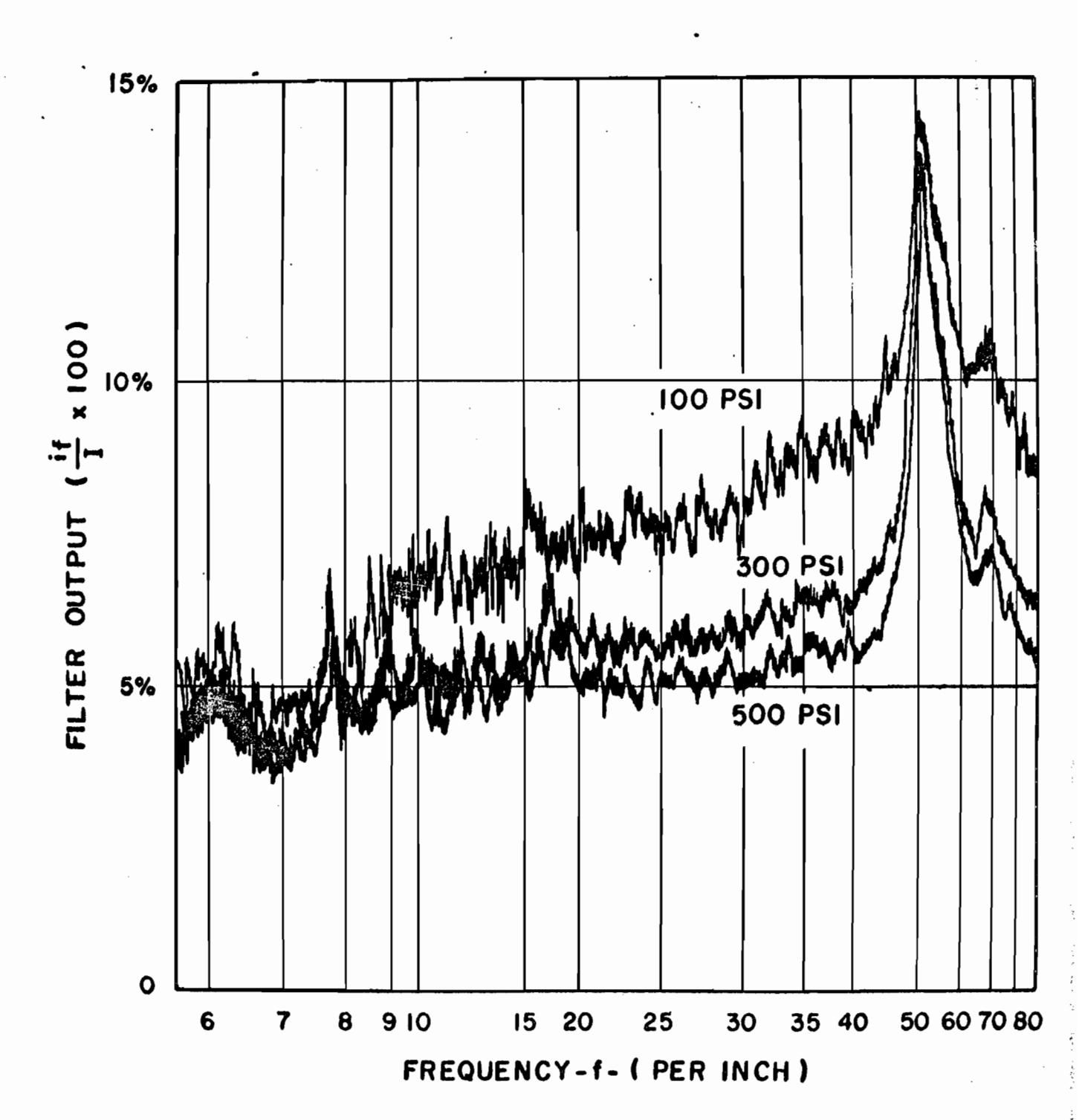


FIGURE 18. EFFECT OF PRISM PRESSURE ON NEWSPRINT HAVING STRONG WIRE MARK (MACHINE DIRECTION)

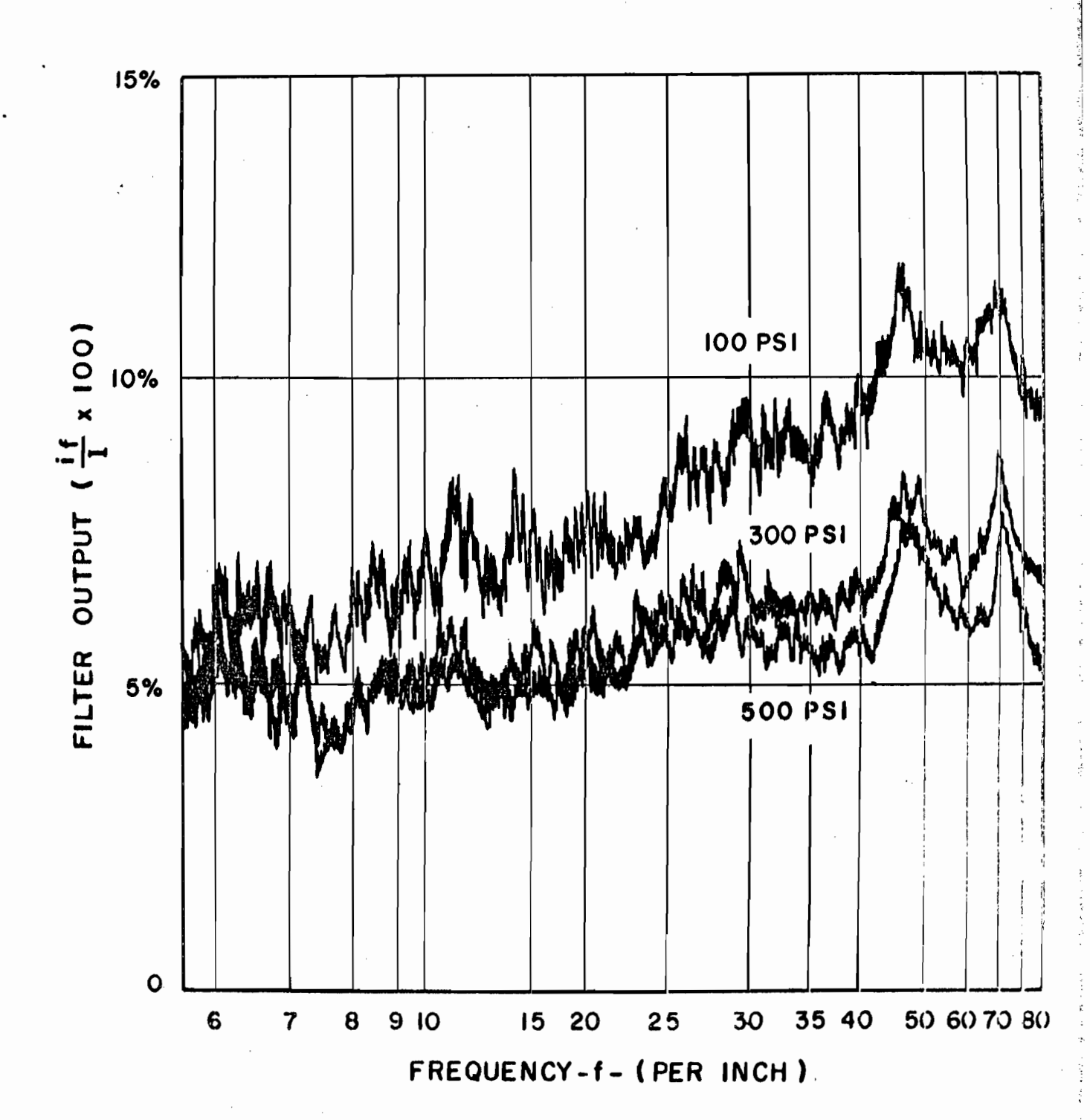


FIGURE 19. EFFECT OF PRISM PRESSURE ON NEWSPRINT HAVING STRONG WIRE MARK (CROSS-MACHINE DIRECTION)

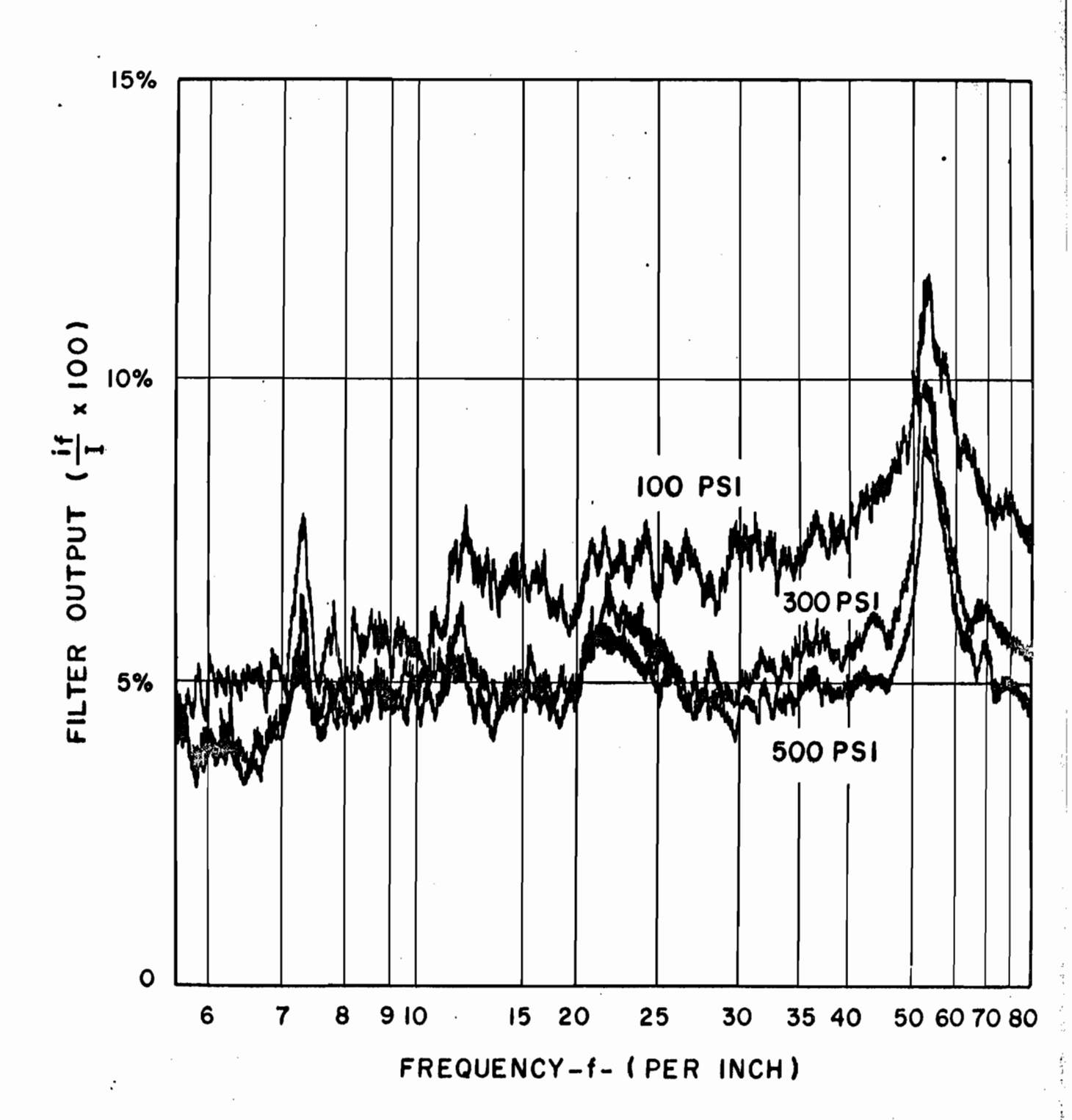


FIGURE 20. EFFECT OF PRISM PRESSURE ON NEWSPRINT HAVING AVERAGE WIRE MARK (MACHINE DIRECTION)

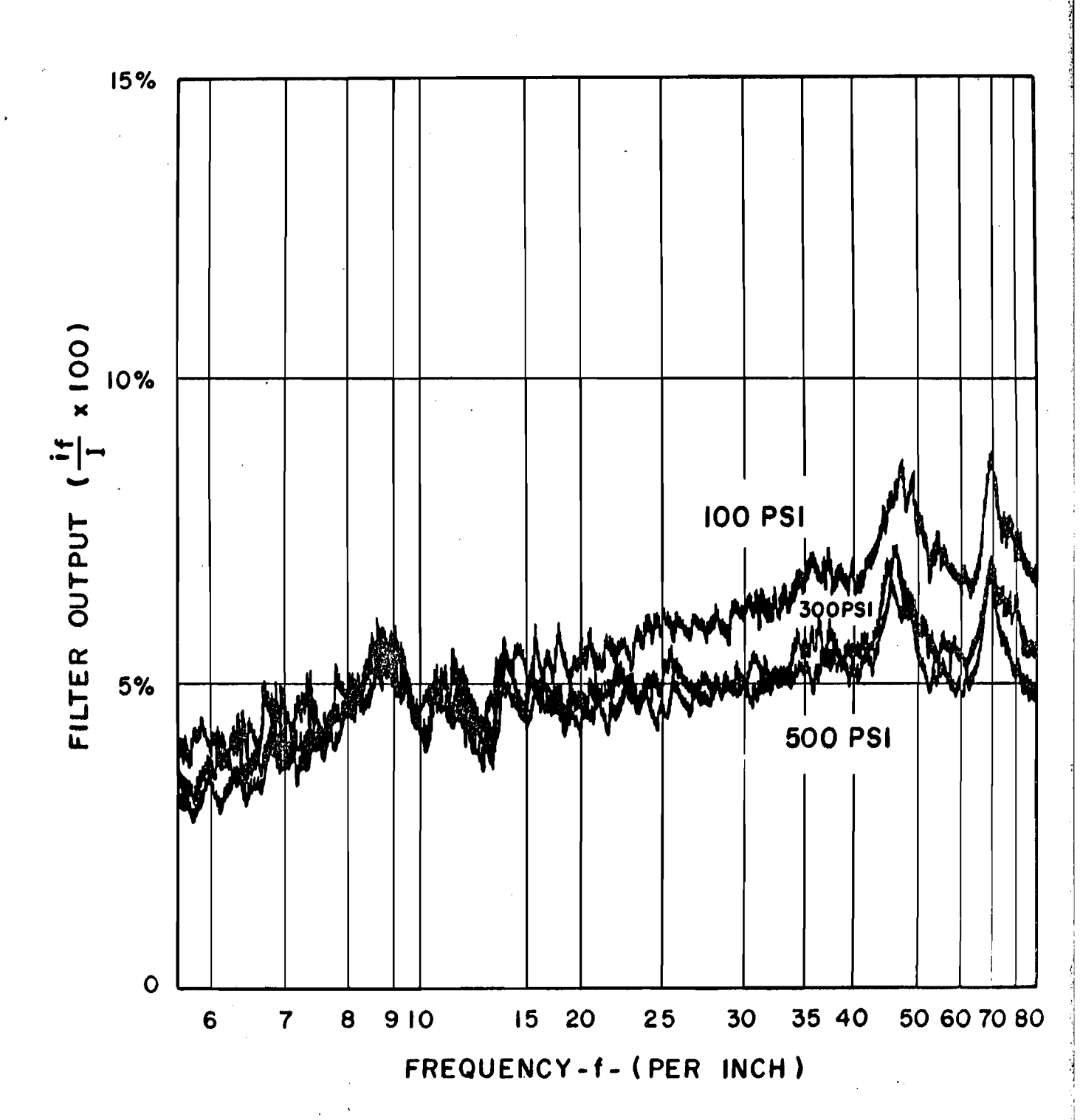


FIGURE 21. EFFECT OF PRISM PRESSURE ON NEWSPRINT HAVING AVERAGE WIRE MARK (CROSS-MACHINE DIRECTION)

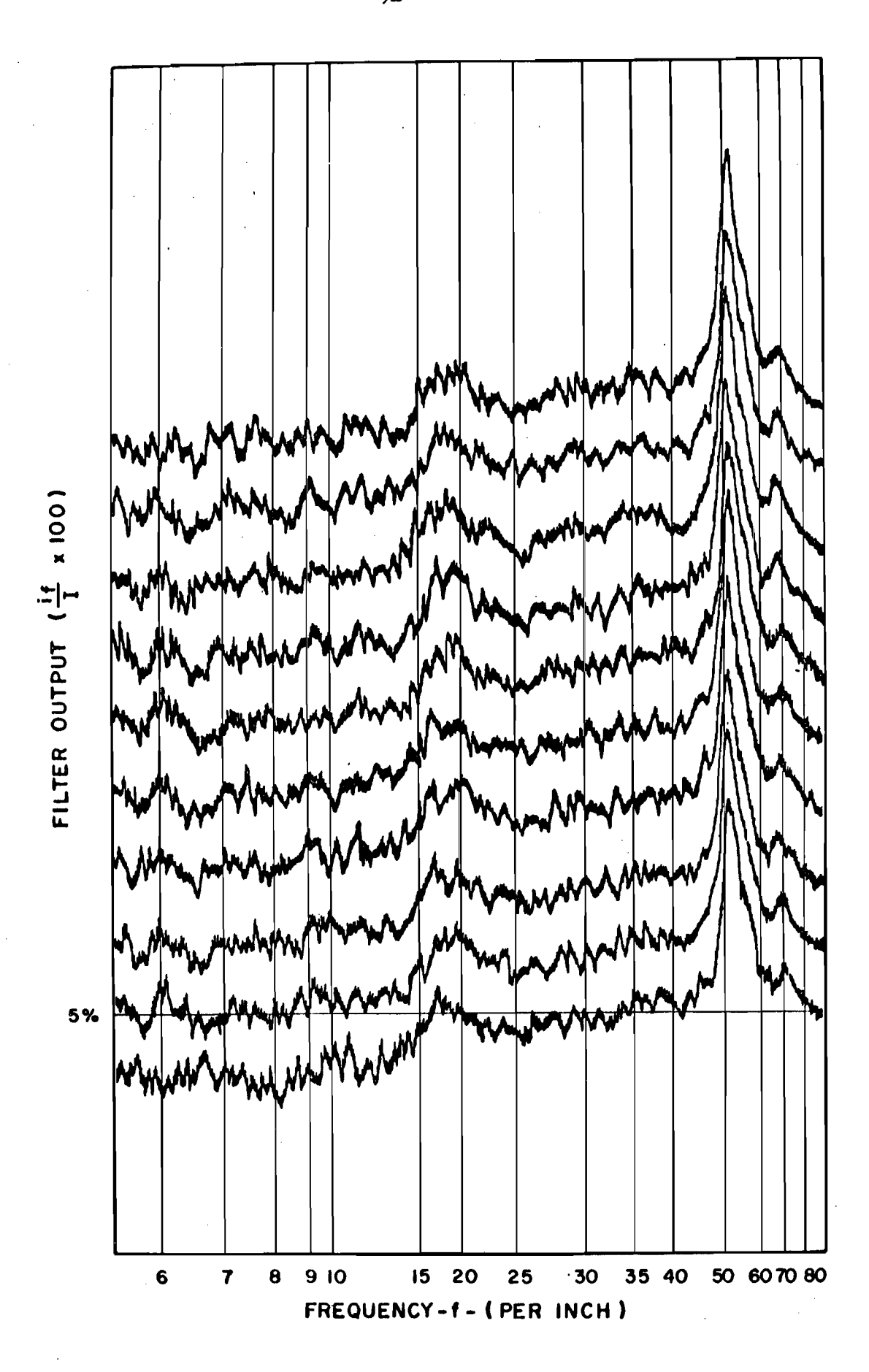
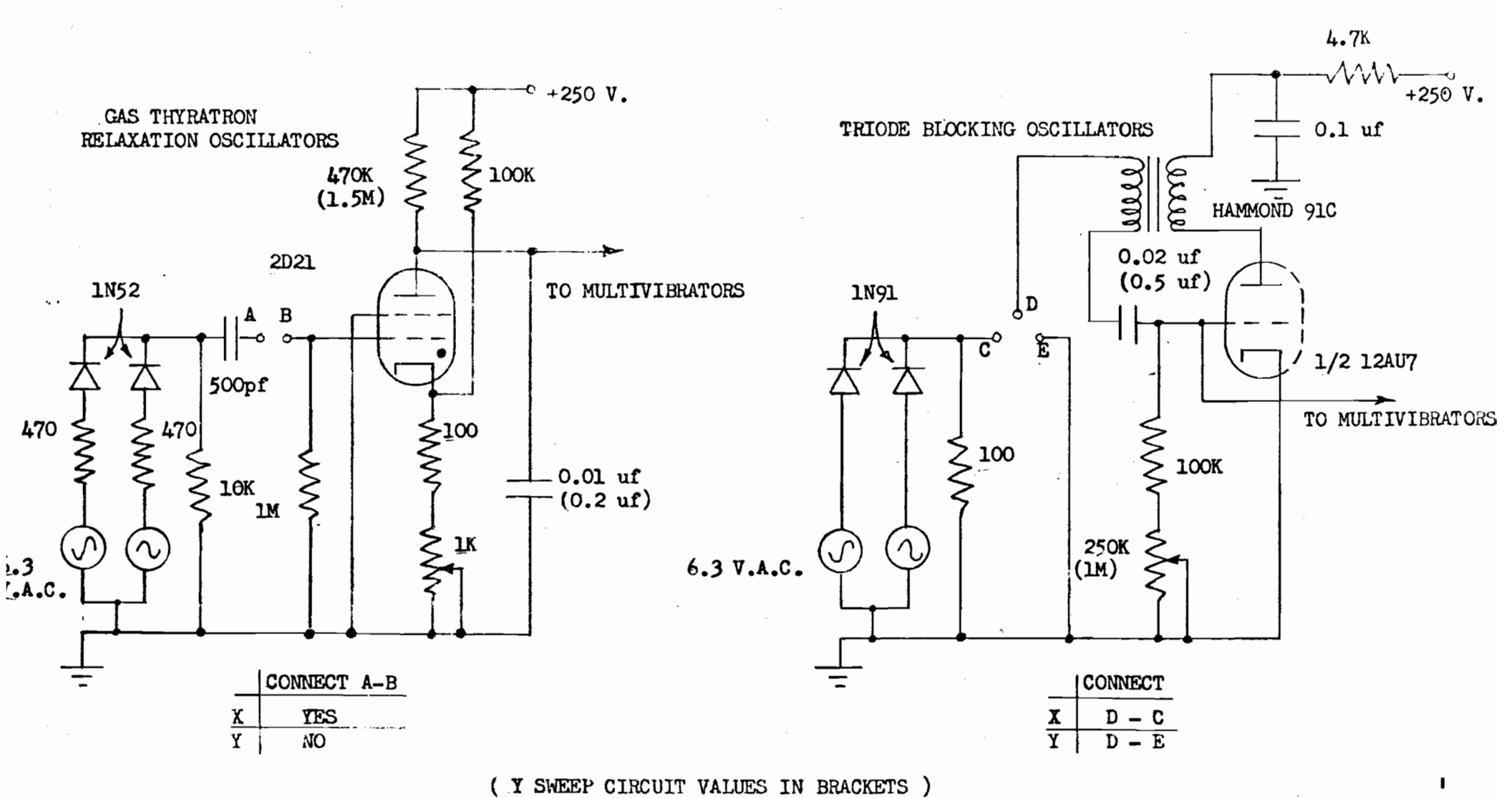


FIGURE 22. REPRODUCIBILITY OF SURFACE ROUGHNESS SPECTRA TAKEN AT A SINGLE LOCATION

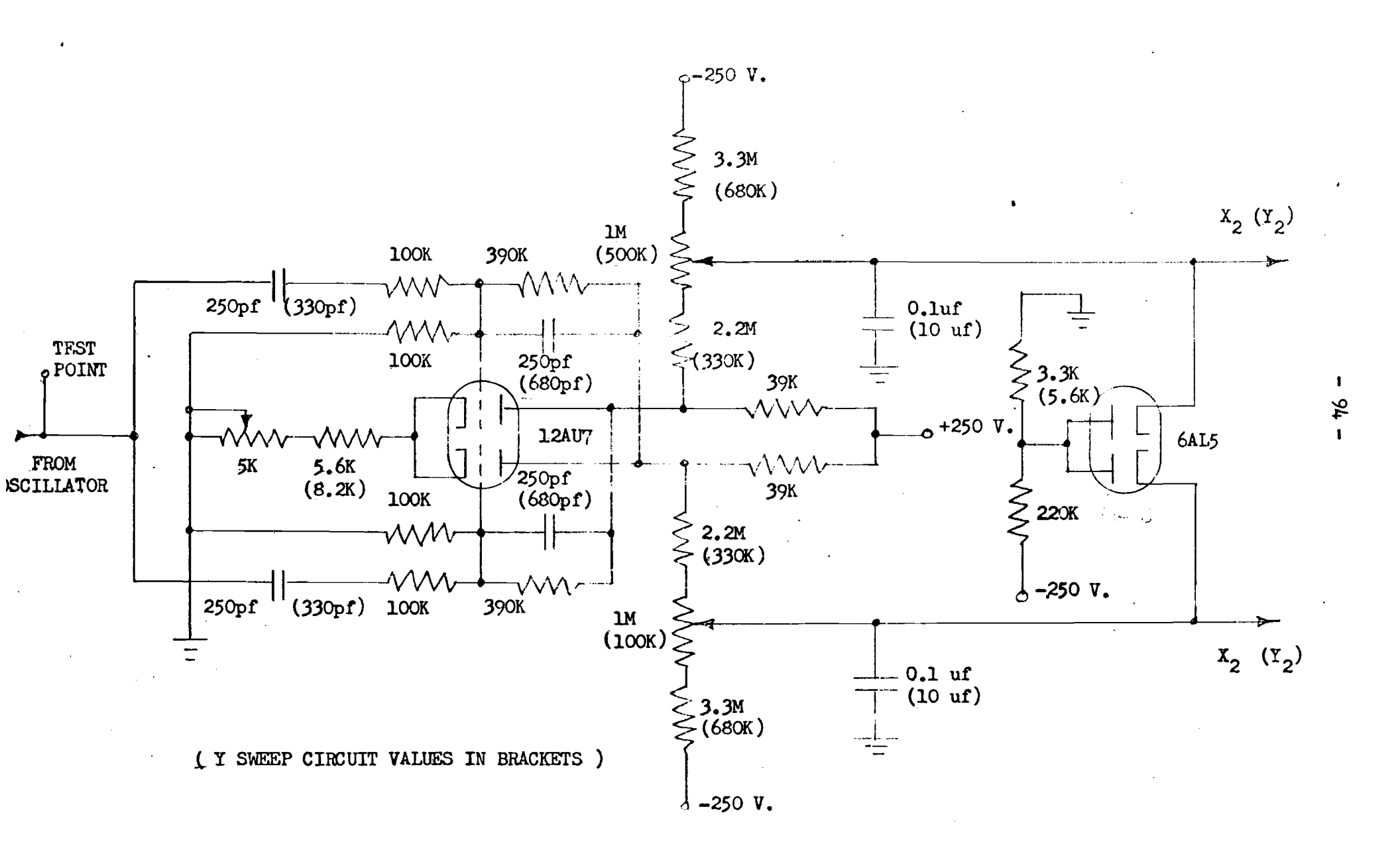
## APPENDIX I : CIRCUIT DIAGRAMS

Figure A:	Relaxation Oscillators - Blocking Oscillators	93
Figure B:	Multivibrators and R-C Integrators	94
Figure C:	X and Y Sweep Circuit Power Amplifiers	95
Figure D:	Control and Bias Circuitry	96
Figure E:	Video Amplifier A <sub>1</sub> and Averaging Amplifier A <sub>3</sub>	97
Figure F:	Filtering Amplifier A2	98
Figure G:	Analysis Circuitry	99
Figure H:	External Calibrator Circuitry	100

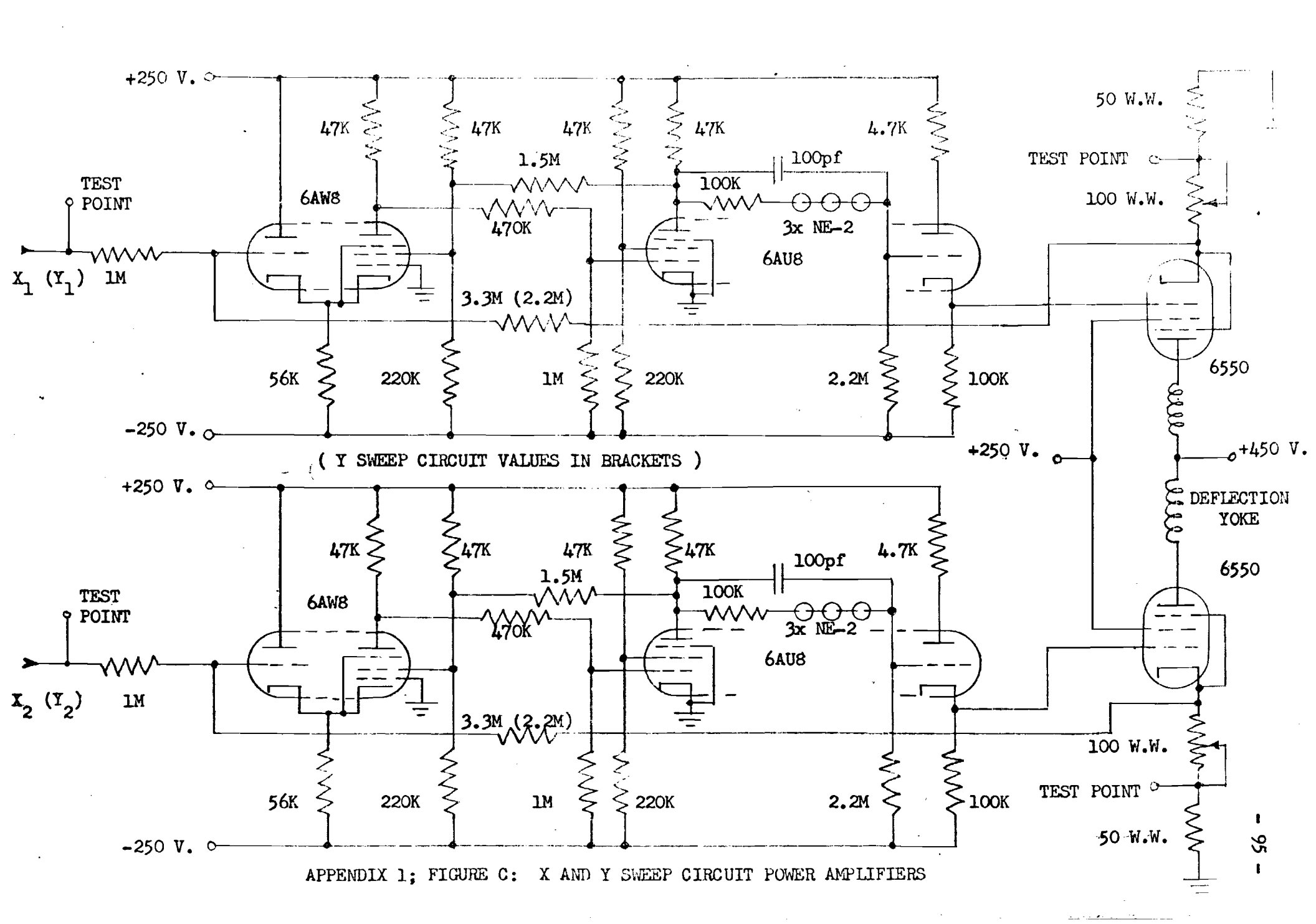


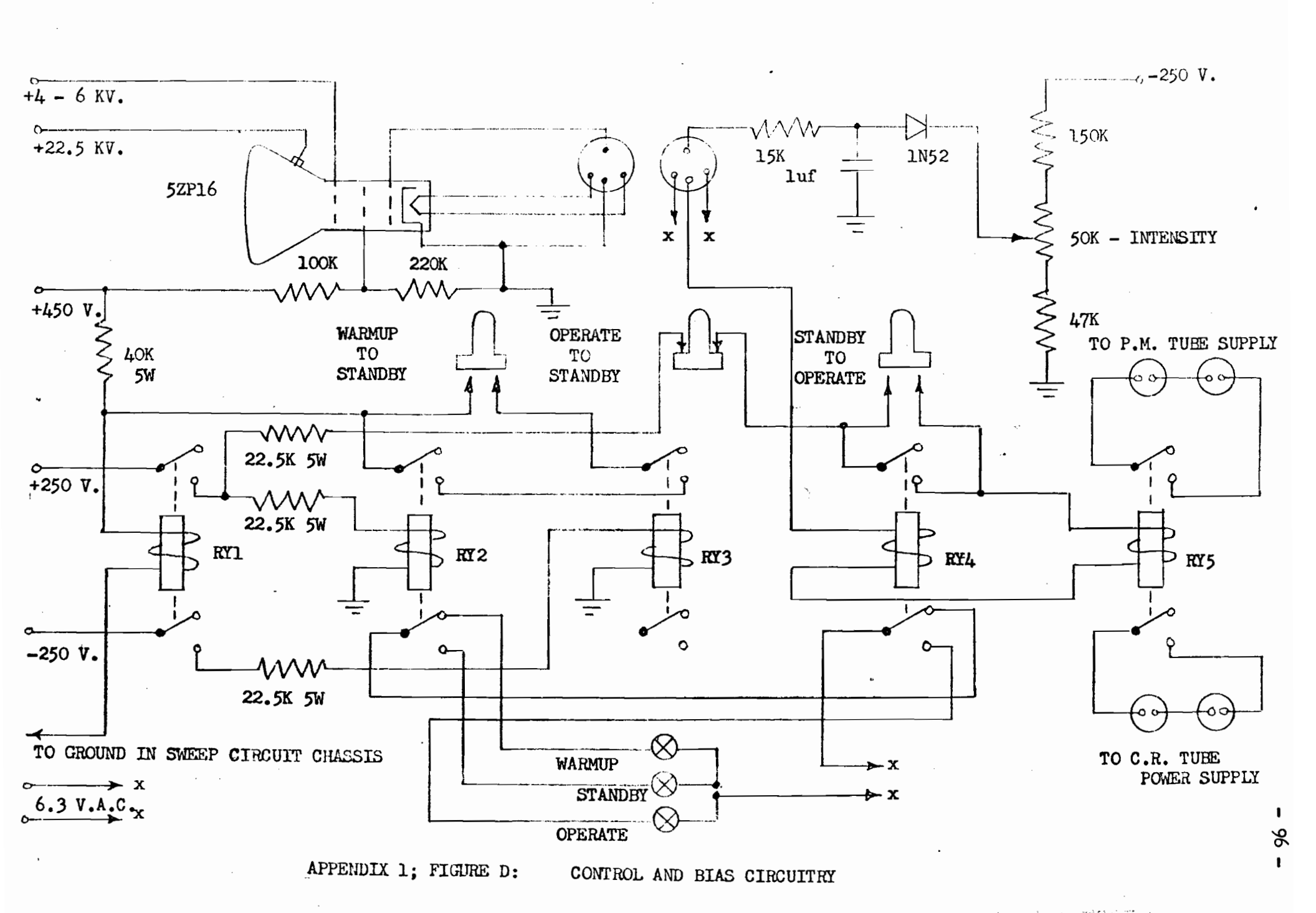
APPENDIX 1; FIGURE A: RELAXATION CSCILLATORS - BLOCKING OSCILLATORS

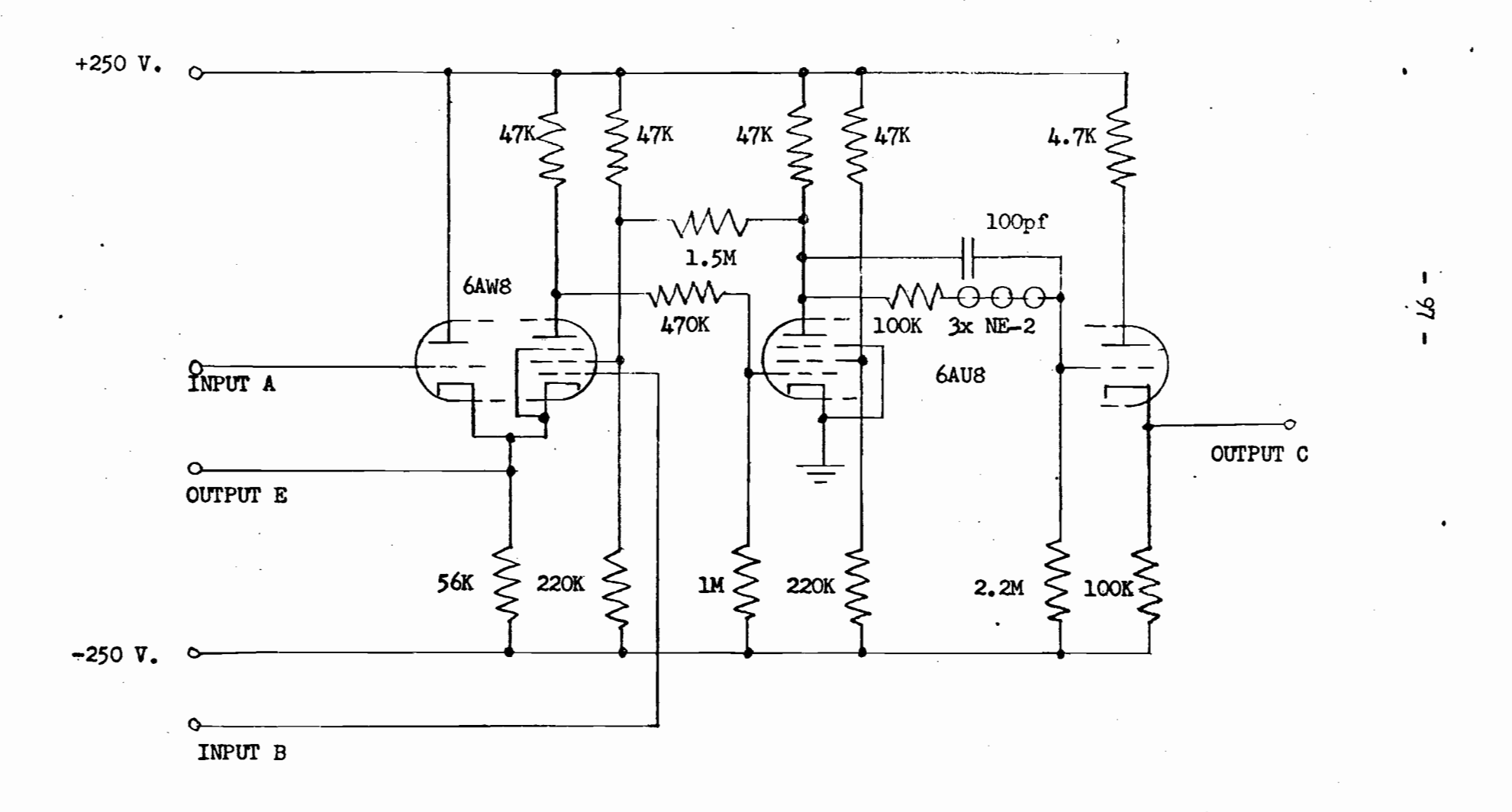
7



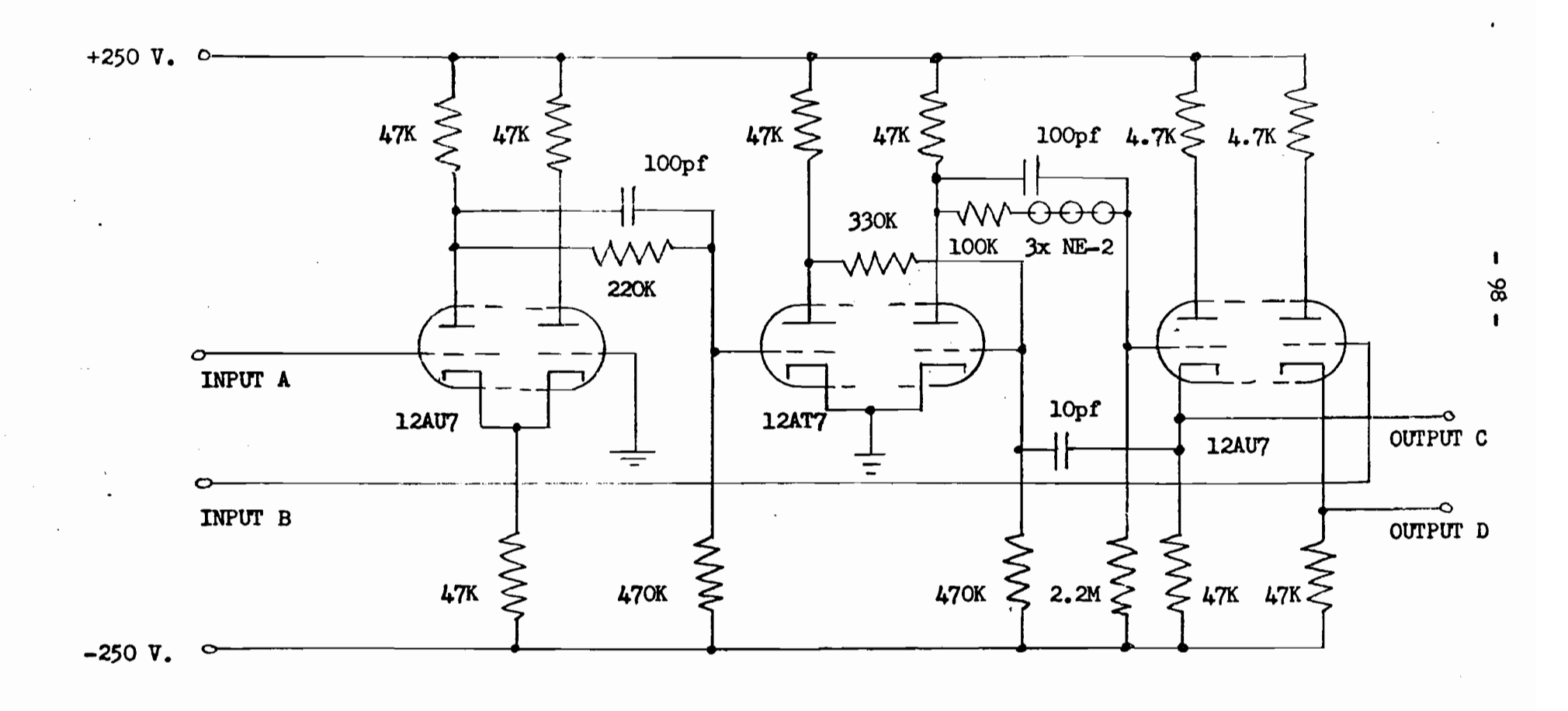
APPENDIX 1; FIGURE B: MULTIVIBRATORS AND R-C INTEGRATORS



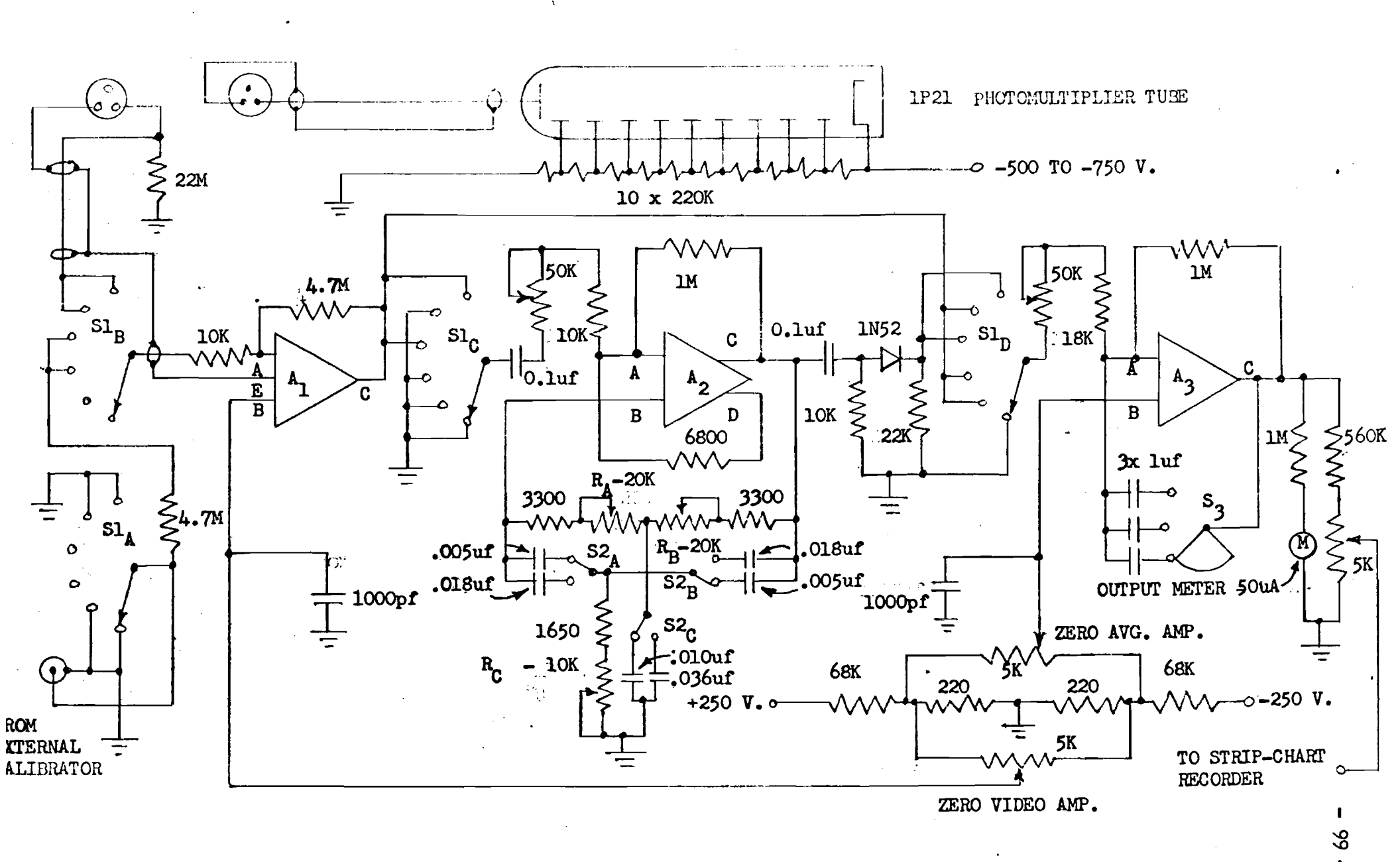




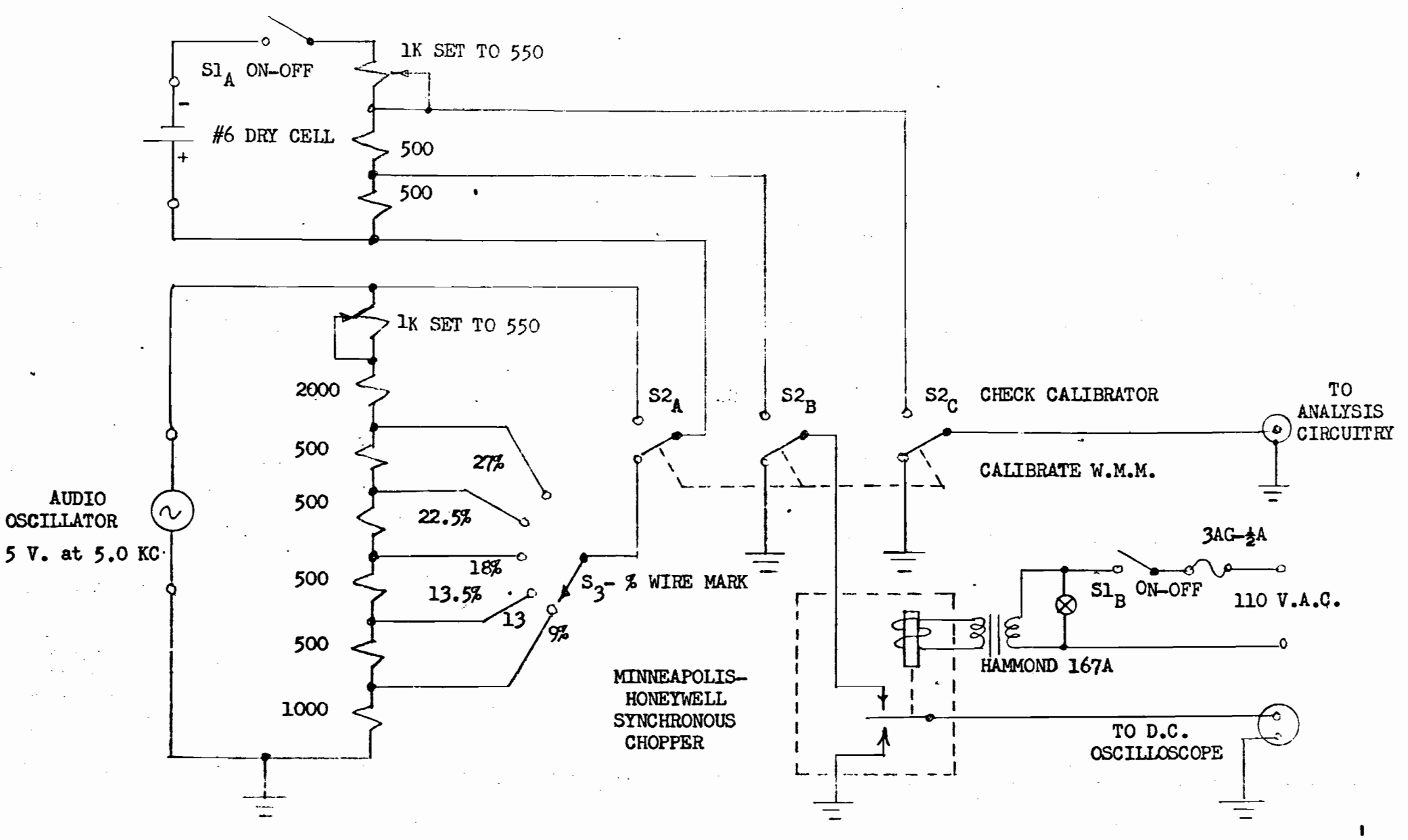
APPENDIX 1; FIGURE E: VIDEO AMPLIFIER A AND AVERAGING AMPLIFIER A



APPENDIX 1; FIGURE F: FILTERING AMPLIFIER A2



APPENDIX 1; FIGURE G: ANALYSIS CIRCUITRY



APPENDIX 1; FIGURE H: EXTERNAL CALIBRATOR CIRCUITRY